

Review Article

Single-molecule fluorescence microscopy review: shedding new light on old problems

Sviatlana Shashkova^{1,2} and Mark C. Leake^{1,2}

¹Department of Physics, Biological Physical Sciences Institute (BPSI), University of York, York YO10 5DD, U.K.; ²Department of Biology, Biological Physical Sciences Institute (BPSI), University of York, York YO10 5DD, U.K.

Correspondence: Mark C. Leake (mark.leake@york.ac.uk)



Fluorescence microscopy is an invaluable tool in the biosciences, a genuine workhorse technique offering exceptional contrast in conjunction with high specificity of labelling with relatively minimal perturbation to biological samples compared with many competing biophysical techniques. Improvements in detector and dye technologies coupled to advances in image analysis methods have fuelled recent development towards single-molecule fluorescence microscopy, which can utilize light microscopy tools to enable the faithful detection and analysis of single fluorescent molecules used as reporter tags in biological samples. For example, the discovery of GFP, initiating the so-called 'green revolution', has pushed experimental tools in the biosciences to a completely new level of functional imaging of living samples, culminating in single fluorescent protein molecule detection. Today, fluorescence microscopy is an indispensable tool in single-molecule investigations, providing a high signal-to-noise ratio for visualization while still retaining the key features in the physiological context of native biological systems. In this review, we discuss some of the recent discoveries in the life sciences which have been enabled using single-molecule fluorescence microscopy, paying particular attention to the so-called 'super-resolution' fluorescence microscopy techniques in live cells, which are at the cutting-edge of these methods. In particular, how these tools can reveal new insights into long-standing puzzles in biology: old problems, which have been impossible to tackle using other more traditional tools until the emergence of new single-molecule fluorescence microscopy techniques.

Introduction

Why do we care about detecting single molecules in cells?

Experimental investigations in the life sciences have traditionally been performed on a population 'ensemble average' level. An example of this is the use of cell cultures, which contain a population of many thousands of cells. A cell population is, in general, intrinsically heterogeneous, even if cells are genetically identical. In other words, different cells exhibit a range of different physical, chemical and biological properties. Such heterogeneity is potentially valuable at a level of the originator species, in that they allow rapid adaptation in a dynamic, fluctuating environment, and so may impart a biological advantage to the ultimate survival of the species [1-3]. Using a population signature as a metric for the physical or chemical status of different cellular parameters is valuable at one level, since it averages out the observations of potential minor and anomalous cells in that population, in effect smoothing out the 'noise'. However, the main problem with this approach is that there may be valuable information hidden in this 'noise'; we run the risk of losing potentially useful data concerning biologically relevant heterogeneity. We potentially limit the extent to which we can investigate 'subpopulations' [4,5].

For example, ensemble average analysis will not pinpoint the drug-resistant bacteria or cancer cells in a general cellular population. When subpopulations are identified, the only way to determine which

Received: 07 April 2017
Revised: 08 July 2017
Accepted: 10 July 2017

Accepted Manuscript Online:
10 July 2017
Version of Record published:
21 July 2017

cells contribute to which group, hence, to separate competing signals, is to analyse the whole population cell-by-cell [6,7]. Population heterogeneity can arise due to environmental alterations affecting the soft matter of biological material [8], as well as through genetic variation that affects gene expression and can invoke fluctuations in various cellular components [9]. Differences in transcriptional regulation affect signal transduction pathways and hence responses to various stress factors, such as pH and oxidative stress. Therefore, an ideal single-cell experiment should be performed under precise environmental control. Moreover, the age of a cell and its phase in the cell cycle may also significantly influence the cell response [4].

Even an apparently simple unicellular organism represents a heterogeneous system on a molecular level [10]. Analysis of the ensemble average of molecular properties results in loss of information concerning any molecular heterogeneity, and may ultimately lead to misinterpretations of the underlying physiological relevance of subpopulations of molecules [11]. Focusing on molecules as the minimal ‘functional’ units in a biological system, single-molecule biophysics research has an important impact on a range of fields of biological investigation. These include fields where biological complexity is rife, such as medical immunology, synthetic and systems biology, but also several others at a more basic mechanistic level, ultimately through an ability to enhance both the effective spatial and temporal resolution of data [11]. Modern techniques [12] enable, for example the probing of the cellular signal transduction dynamics directly [13], which facilitates a deeper and more precise understanding of important biological processes, e.g. the human immune response, gene expression and cellular differentiation. One of the most important techniques used currently in single-molecule biophysics research is, unquestionably, fluorescence microscopy [14,15].

Identification and investigation of molecular subpopulations within the cell enables us to study not only cellular responses but also the precise underlying molecular mechanisms. Arguably, the first clear demonstration that single-molecule fluorescence microscopy could yield insight which were genuinely unanticipated from bulk ensemble average measurements was reported in 1998. Here, the researchers used the native photoblinking behaviour of the common metabolite FAD inside a binding site of the enzyme cholersterol oxidase to demonstrate that its activity could be affected by a type of ‘molecular memory’ stored in the molecular conformation [16]. Single-molecule fluorescence microscopy approaches since then have uncovered many fundamental molecular scale biological processes that were previously not studied primarily due to the limitations imposed by population methods, including studies of the bacterial flagellar motor rotation [17–21], protein folding, translocation and movement [11,22–25], signal transduction [26], biopolymer mechanics [27–32], DNA replication and remodelling [33–37], oxidative phosphorylation [38–41], as well as biomedically relevant areas such as the probing of processes relating to infection and general pathology [42–44], cell division mechanisms [45], mitochondrial protein dynamics [46], viral infection processes [47], endocytosis and exocytosis pathways [48], osmolarity receptor dynamics [49], cell wall synthesis [50], and structural dynamics of DNA [51]. This list above should not be taken as exclusive nor exhaustive, but rather we present it here to exemplify the very wide range of biological processes to which single-molecule fluorescence microscopy tools have been applied.

One of the primary requirements for all the single-cell/single-molecule approaches is the ability to faithfully detect small signals over sometimes relatively large noise levels [52]. Combining improvements in a range of different approaches, such as minimizing the sample volume, engineering better photostability for newer variants of fluorescent proteins, and improving the sensitivity of camera detectors, have resulted in higher detection levels of photon signals for fluorescence emission, though still there are limitations due to poor signal-to-noise ratios when sampling at very high imaging rates. Various analytical tools have been developed to improve the signal-to-noise ratio, such as automated methods of ‘segmentation’ of cellular images [53,54], robust software algorithms for the tracking of fluorescently labelled molecules [55–57], and stoichiometry analysis of molecular complexes which those tracked molecules form. We steer the reader to recent comprehensive reviews that discuss these different approaches on how to increase the fidelity of signal detection over background noise [52,58].

Fluorescence and fluorescent proteins

The physical process of fluorescence occurs when a photon of light is absorbed by a ‘fluorophore’, which may be an atom or a molecule, and consequently re-emitted as a photon with a longer wavelength. The loss of energy occurs due to vibrational processes which result from oscillations between the atomic/molecular orbitals due to the perturbation of a different negative electron charge distribution relative to the positively charged nucleus. Upon standard ‘single photon excitation’, light absorption of a single photon (of light) occurs which results in a ground state electron in the fluorophore undergoing an excitation transition to a higher energy state, in a process characterized by a time scale of $\sim 10^{-15}$ s. Following this relatively transient state, the excited electron loses energy through vibrational losses over

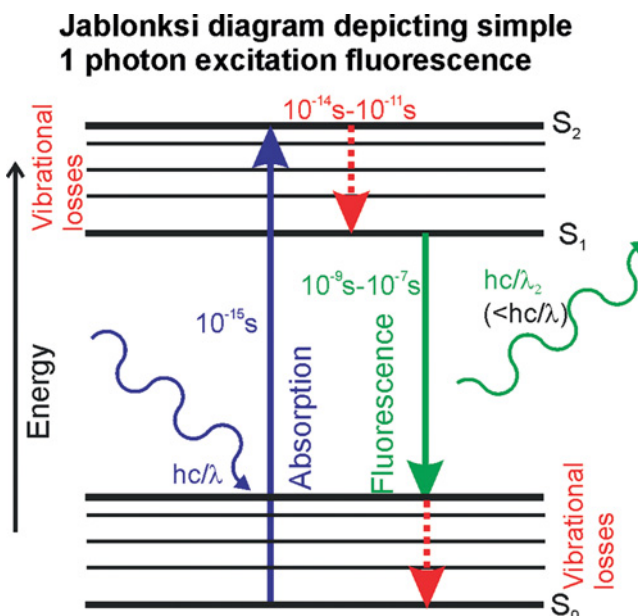


Figure 1. Jablonski diagram

An electron of a fluorophore at the ground state (S_0) receives energy from the absorption of a single photon of light which results in an excitation transition to a higher energy state (absorption). When the excited electron relaxes to the ground state, following vibrational losses, energy, lower than the incident photon and thus with a higher wavelength, is emitted as a single photon which causes fluorescence.

a time scale of 10^{-14} – 10^{-11} s. The electron then undergoes an energy transition back to the ground state, characterized by a time scale of 10^{-9} – 10^{-7} s, accompanied by photon emission, whose wavelength is longer than the incident wavelength (i.e. has a smaller associated energy). Jablonski [59] described the different energy states and transitions between them in a useful pictorial form called Jablonski diagram (Figure 1). Although the physical process of fluorescence was properly formulated by the British scientist Stokes et al. [60], it was more than half a century later that the first operational fluorescence microscope was developed, reported in 1911, which obtained the relatively standard design as we know it today only in 1967 [61].

In 2008, the Nobel Prize in Chemistry was awarded jointly to Osamu Shimomura, Martin Chalfie and Roger Y. Tsien for the ‘discovery and development of green fluorescent protein, GFP’ [62]. GFP had been isolated from the jellyfish *Aequorea victoria*, described in an article in 1962 [63]. A step change came when the GFP gene was sequenced in the early 1990s, accompanied by developments in molecular cloning technologies enabling the integration of its DNA directly into DNA in other organisms. Nowadays, it is an invaluable tool which is widely used as a fluorescent tag and can be relatively easily integrated into the genome. GFP is a β -barrel protein consisting of 11 β -sheets and an α -helix, composed of 238 amino acids residues in total. The wild-type GFP chromophore is encoded by the Ser⁶⁵-Tyr⁶⁶-Gly⁶⁷ sequence which forms a heterocyclic photoactive state spontaneously through the processes of intramolecular autocatalytic rearrangement and subsequent oxidation [64]. This final oxidation stage is crucial for the protein to function as an active fluorophore.

Numerous mutations of wild-type GFP have now been generated, with one of the principle aims of improving its biophysical characteristics. Photostability and fluorescence output increases were achieved by using an S65T mutation [65], while the A206K was developed to prevent self-oligomerization [66], and various colour mutations were added, including, for example blue Y66H, cyan Y66W and yellow T203Y [67] variants. Standard fluorescent proteins will undergo irreversible photobleaching after a characteristic time interval when excited to fluorescence, most likely to be due to the accumulation of free radicals in the surrounding water solvent formed from the lysis of water molecules upon absorption of photons of light, and their subsequent chemical damage to the fluorescent protein structure. Standard fluorescent proteins cannot therefore be tracked longer than their photobleaching point, which thus limits their application in long time scale experiments.

Certain newly engineered fluorescent proteins, e.g. mEos [68], Dendra [69] and KikGR [70] can be photoactivated and undergo irreversible photoconversion from green to red emitting state upon irradiation with UV light [71,72]. Although such approaches potentially can appear to extend the lifetime of a tracking experiment in which

proteins can be photoconverted before they bleach, there is no intrinsic improvement as such to photostability in these proteins. Monomeric forms of these proteins [73,74] as well as different variants of photoconvertible proteins with enhanced features have also been designed. For example, mMaple protein exhibits reversible photoconversion under certain conditions [75], with yellow-to-cyan (EYFP-to-CFP) photoconversion upon green light illumination [76], and cyan-to-green photoswitch of PS-CFP2 [18]. The fluorescent protein mOrange undergoes orange-to-red activation upon illumination with blue light (typically using the common laser line with wavelength 488 nm), which is thus less harmful for live cells compared with UV-convertible proteins in regard to photodamage effects [77]. Photoconversion can be used stroboscopically to divide up the finite photon budget prior to photobleaching (i.e. acquiring fluorescence images over extended time intervals instead of continuously illuminating samples), which has been used to monitor complex live samples such as developing embryos for up to several hours [78]. Another type of fluorescent protein, phytochrome-based near IR fluorescent proteins (iRFP), has been developed recently [79]. Compared with conventional fluorescent proteins, such as GFP, iRFP has a higher effective signal-to-noise ratio and allows imaging deeper into tissues due to smaller elastic scattering effects at higher wavelengths of electromagnetic radiation, relevant for applications in live-animal or excised-tissue models.

Some fluorescent proteins have a characteristic time over which they change their emission wavelength from blue to red based on the chromophore maturation time. Such proteins can be used, therefore, as fluorescent timers, such as to study protein transport. For example, an mCherry-derived monomeric variant with various timing behaviours has been used for probing the kinetics of protein trafficking [80].

Fluorescent probes may be added to a protein of interest directly or via linkers, such as SNAP- and HALO-tags. Here, the encoding DNA for a protein probe is first genomically fused next to the protein under investigation, technologically similar to the approach used in developing fluorescent protein fusion constructs. In most applications of HALO/SNAP, this probe consists of a DNA repair protein (for SNAP) or a haloalkane dehalogenase enzyme (for HALO) [81,82]. The cell can then be incubated with a secondary probe which is fluorescently labelled with a bright organic dye fluorophore. The secondary probe is designed to bind to the primary protein probe. The use of these tags avoids 'direct' fluorescent protein labelling, which might impair their physiological behaviour due to steric hindrance. This methodology enables a far brighter and more photostable fluorophore to be used compared with conventional fluorescent proteins. Since the localization precision improves with the brightness of the fluorophore used (roughly with a reciprocal dependence on the square root of the brightness) the use of a brighter dye facilitates improvements in localization precision for determining the position of individual fluorophores. This method also implies a potential improvement to temporal resolution in ultimately enabling faster sampling for a given spatial localization precision. That being said, the primary probes for SNAP and HALO are themselves reasonably large whose molecular weight is only ~40% less than that of fluorescent proteins of ~28 kDa [5], and so a potential steric hindrance effect is still present. Also, the efficiency of labelling during the secondary probe incubation step is sometimes difficult to achieve as the primary protein probe is often not easily accessible, e.g. the primary probe protein is deep inside a cell and thus there are technical issues in how to deliver the secondary probe to these regions. However, this approach has resulted in significant advances in super-resolution imaging of accessible cell surface structures, such as the cell wall architecture of bacteria [83].

Main techniques and applications of single-molecule fluorescence microscopy

A potted history of the development of single-molecule fluorescence microscopy

The first report of the inference of the presence of single molecules using fluorescence microscopy came as early as 1961 from the work of Boris Rotman. In that study, the product of an enzyme-catalysed reaction was labelled with a fluorescent dye, and since each single enzyme molecule resulted in the manufacture of several thousand product molecules, this intrinsic 'chemical amplification' resulted in the ability to detect a fluorescent signal from aqueous droplets of the reaction solution immobilized on to a mica surface [84] using relatively insensitive camera technology compared with those we use today. The direct detection of single molecules using fluorescence microscopy was first reported in 1976 from the work of Thomas Hirshfeld in which molecules of the protein globulin were labelled with, on an average, several tens of a bright organic dye fluorophore molecule, and these fluorescently labelled particles could be detected as they were flowed past a photodetector in aqueous solution. The first report of detecting single fluorescent dye tags directly, which used a similar experimental approach, came in 1990 [85].

Following these seminal developments, the 1990s brought forth many important developments in regard to improving the spatial resolution of detection of single molecules using fluorescence microscopy. It may be useful for us now to consider some of the basics about optical resolution theory. Fluorophores which are visualized in the 'far-field' regime (i.e. there is a distance of several wavelengths of light between the fluorescence source and the detector) exhibit diffraction. In a light microscope, the apertures through which light propagates are in general circular and for these the diffraction pattern which results is known as an Airy ring or disk, the shape of which is determined by the so-called point spread function (PSF) of the microscope system.

The intensity profile of an Airy ring pattern can be described analytically by using a mathematical function called Bessel function – this 2D relation consists of a central circular region of bright intensity surrounded by alternating minima and maxima in concentric rings of increasing radius from the centre. The diffraction angle of the first dark ring, θ , mathematically satisfies the equation $\sin\theta \approx 1.22\lambda_m/2r = 0.61\lambda_m/r$, where r is the radius of the circular aperture in question and λ_m is the wavelength of the light in the imaging medium. If the circular component is an objective lens of focal length f , then the lateral distance d in the image plane from the optic axis to the first dark ring is given by the relation $f\sin\theta_{\max}$, where θ_{\max} is the maximum allowed diffraction angle corresponding to the first dark ring emerging from the circular aperture. If the imaging medium has a refractive index n , then $\lambda_m = \lambda/n$ where λ is the wavelength of the light in vacuum. Rearranging these relations thus indicates that $d = 0.61 \lambda/n\sin\theta_{\max} = 0.61 \lambda/NA$, where NA is the numerical aperture of the objective lens.

If there are two Airy ring patterns overlapping such that the centre of one just overlaps with the first dark ring of the other, then their separation will be equal to d . This is the basis of the 'Rayleigh criterion' of the optical resolution limit. It approximates to the minimal distance at which two points can be *distinctly* detected in the far-field regime in a light microscope. In 1873, Abbe [86] described that the optical resolution of the light microscope is limited by the diffraction properties of light, through the formulation (known as 'Abbe's limit') of $\lambda/2NA$, by consideration of *rectangularly* shaped apertures in a diffraction grating (as opposed to a circular aperture), and for these the equivalent diffraction angle is given as $\lambda_m/2D$ where D is the aperture width.

Optical imaging techniques which render spatial information at a precision better than the optical resolution limit are known as 'super-resolution' microscopy methods. These have added an exceptional level of insight into challenging biological questions, exemplified in 2014 when Eric Betzig, Stefan W. Hell and William E. Moerner were jointly awarded the Nobel Prize in chemistry 'for the development of super-resolved fluorescence microscopy' [87]. Development of a range of super-resolution techniques have been invaluable for single-molecule fluorescence microscopy, enabling scientists to break the optical resolution limit to study the functional localization and interactions of biological substructures at the level of single molecules down to nanoscale precision [10]. Today, these varied super-resolution methods enable us to obtain genuinely new insights into fundamental biological mechanisms which have been long-standing questions in the field: the 'old problems' of the title of this review that were previously intractable due, primarily, to technical limitations imposed by conventional ensemble average methods.

Arguably, the simplest way to achieve super-resolution is to avoid imaging in the far-field regime, *per se*, but rather perform *near-field* imaging (i.e. where the fluorescent source and detector are separated by less than a few wavelengths of light) since, then one is not subjected to significant optical diffraction effects. In this regard, the first experimental application of super-resolution light microscopy was reported in 1981, as the technique called total internal reflection fluorescence (TIRF) microscopy [88]. Although resulting fluorescent samples being subjected to standard diffraction-limited resolution in the lateral plane of the microscope (i.e. the focal plane), TIRF uses near-field excitation axially by generating an evanescent field which delimits this axial illumination to a length which is shorter than the standard optical resolution limit. The first single-molecule biological application of this technology was reported in 1995 involving *in vitro* experiments to monitor ATP turnover by single myosin molecules [89], while the first single-molecule fluorescence microscopy imaging in live cells also used TIRF, reported in 2000, which investigated epidermal growth factor (EGF) receptors and ligand binding using fluorescently labelled EGF [90].

Another early developed near-field, single-molecule fluorescence technique used scanning near-field optical microscopy (SNOM or NSOM). Here, the laser excitation field operates over a length scale shorter than the optical resolution limit in being limited by the size of the probe tip down to just approximately 10 nm, first demonstrated on single fluorescent molecules in 1993 [91]. A modification of this approach enabled excitation of a donor fluorophore in the non-radiative technique of single-molecule FRET (smFRET), reported first in 1996 [92]. Here, not only is the excitation field smaller than the optical resolution limit, but also FRET only operates over a length scale comparable with the physical size of the molecular orbitals of the donor and acceptor fluorophore dyes employed of approximately 0–10 nm.

Another commonly used super-resolution method today involves localization microscopy. This is performed in the far-field regime and relies on the fact that the centre of an Airy disk pattern is the best estimate for where the actual

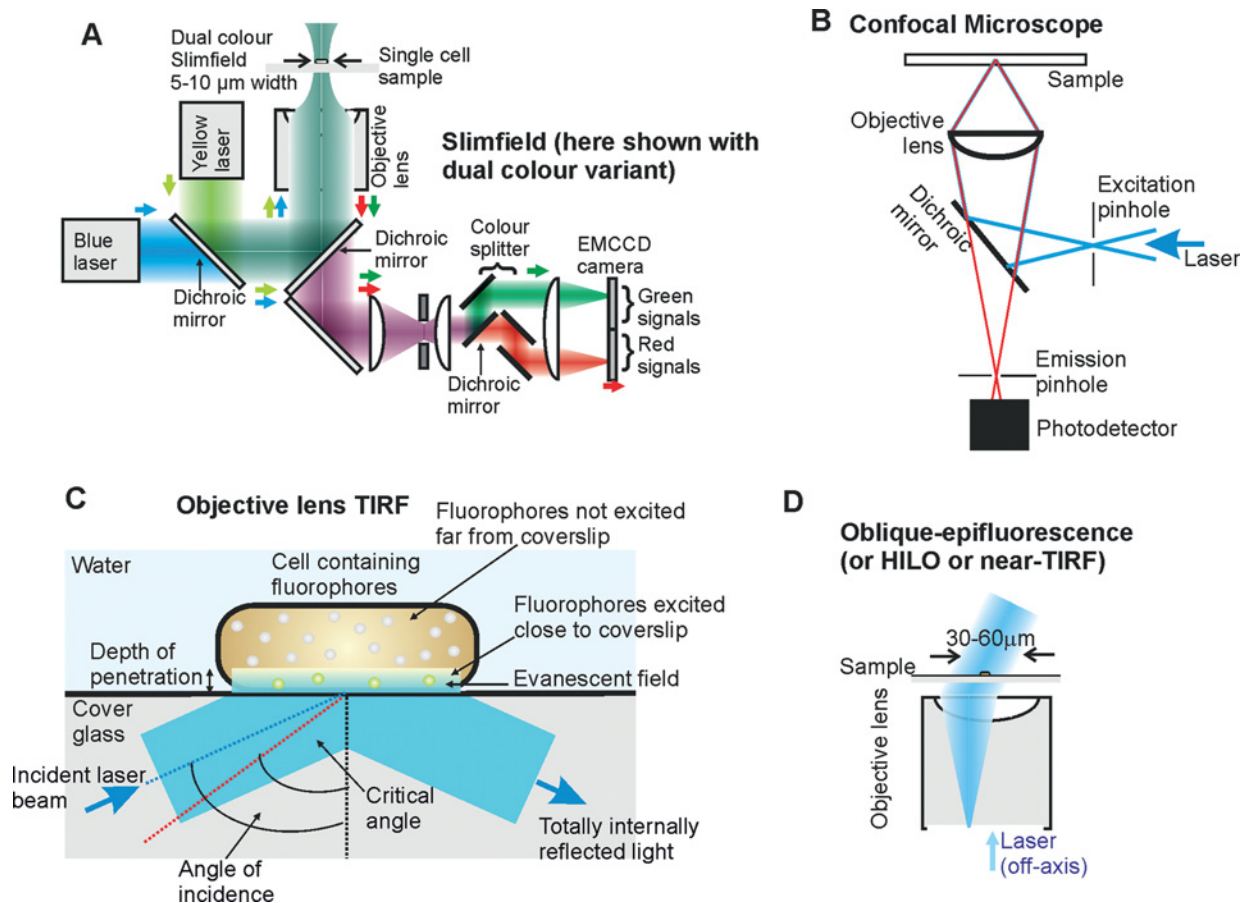


Figure 2. Schematic representation

Of: (A) Slimfield imaging; (B) a confocal microscope; (C), TIRF showing the illumination of fluorophores close to the glass coverslip surface (detailed explanation is provided in the text); (D) HILO microscopy.

fluorescence-emitting dye molecule is in space. Thus, if Airy disk patterns from a population of many dye molecules are separated by greater than the optical resolution limit then, we can apply mathematical fitting methods to estimate where their fluorescence emission ‘centres’ actually are. This approach was used to monitor the diffusion of single fluorescent molecules to a precision roughly to an order of magnitude better than the optical resolution limit, first reported in 1996 by Schmidt et al. [93]. Here, a fitting algorithm was used which approximated the central intensity of the Airy disk pattern using a Gaussian function in a method applied to micron-sized beads used as a probe on single kinesin molecule translocating on microtubules tracks, reported from the lab of Sheetz et al. in 1988 [94].

There have been myriad super-resolution studies published to date which utilize localization microscopy approaches, but arguably the most recent developments with this basic method have involved improvements using probabilistic methods of single particle tracking. For example, the so-called Bayesian approaches to infer the detection and tracking of fluorescently labelled particles [95], and improvements to the speed of tracking. For instance, techniques which reduce the size of the illumination area of excitation, like slim-field or narrow-field fluorescence microscopy, have been developed [96]. Such methods can enable tracking of single fluorescent proteins over very rapid millisecond time scales which significantly reduces motion blur of diffusing fluorescently labelled molecules in different compartments of live cells (Figure 2A), especially in the cytoplasm in which the viscosity is relatively low and so the rate of diffusion is relatively high [33]. These rapid imaging single-molecule fluorescence microscopy techniques may also be combined with convolution analysis of live cell fluorescence images to determine the copy number of proteins in a single cell, and indeed in separate cellular compartments [97]. Most super-resolution techniques, however, are mainly based on conventional fluorescence and confocal microscopy principles [98], but have resulted in huge advances in our knowledge of the biosciences, in particular concerning how processes operate in functional, living cells.

This 'intrinsic' optical resolution limit can also be broken, however, even in a far-field regime. In the 1980s, a Russian scientist Okhonin [99] patented the first super-resolution microscope based on 'stimulated emission depletion (STED)', however, experimentally the principle was first demonstrated only later by Hell et al. [100], apparently unaware of Okhonin's earlier insight judging from the lack of reference to Okhonin's patent.

In the sections below, we outline some of the specific details concerning the modern light microscopy techniques which enable single-molecule fluorescence-based detection in particular.

Confocal microscopy

The conception of confocal microscopy (Figure 2B) is often attributed to Minsky [101,102], who published an initial patent for a confocal microscope in 1961. This method, also called confocal laser scanning microscopy (CLSM), enables in-effect optical sectioning through a biological sample. The word 'confocal', implying 'having the same focus', refers to the presence of two pinholes which are conjugated in the same image plane. One of them is used for spatial filtering of the excitation laser beam by removing side lobes at a position where the laser beam is focused, and the other for the emitted light path, which eliminates a significant proportion of stray signals coming from above or below the focal plane. The first practical working confocal microscope was built by the pioneering efforts of Eggar and Petráň [103], whose first biological application was reported in 1967 to visualize unstained nerve cells in the brain.

The basic method for confocal microscopy involves scanning of the specimen by moving either the stage in vertical and horizontal directions (Minsky's method) or the laser beam in more modern systems [104]. Confocal microscopy can significantly improve the effective signal-to-noise ratio for detection by removing out-of-focus fluorescence. For instance, confocal fluorescence microscopy was used in studies of DNA repair processes through observing bubble DNA/GFP-tagged nucleotide excision repair (NER) protein interactions under physiological conditions [105]. Development of a novel video-rate confocal microscope allowed monitoring the diffusion of *Dictyostelium discoideum* cAMP receptors on basal and apical surfaces [106]. Many recent single-molecule studies utilize a confocal microscope primarily simply to generate a 'confocal excitation volume' (i.e. a diffraction-limited, 3D-focused laser 'spot' in the sample) to act as the illumination source to excite fluorescently tagged molecules which are then detected by other imaging techniques. Several attempts to improve resolution and signal-to-noise ratio of CLSM have been made recently, including the so-called Airy scan in which each pixel detector element on a camera can be treated as a pinhole, which has enabled, for example, the determination of the shape and dimensions of virus particles [107,108].

TIRF

TIRF is now one of the most frequently used imaging methods in single-molecule fluorescence microscopy. The method is based on total internal reflection of incident excitation light from a glass–water interface, such as between a glass coverslip/slide and a water-based physiological buffer (Figure 2C). When light which is incident on an interface in refractive index, n , such as that between water ($n=1.33$) and glass ($n=1.52$), then refraction of the beam will in general occur at angles of incidence not normal to the interface, deviating the direction of the light, unless the angle of incidence is high enough such that the refraction angle is equivalent to 90° or more. The angle of incidence at which the angle of refraction is exactly 90° is known as the 'critical angle', and is simply given by the relation: $\sin^{-1}(n_{\text{water}}/n_{\text{glass}})$ or approximately 62° . At angles of incidence greater than this, total internal reflection of the incident beam occurs at the interface, instead of transmission through the water. A caveat of this is that some of the light is allowed to extend beyond the interface into the water as an 'evanescent field', whose intensity falls off exponentially with distance from the glass/water interface.

Although the evanescent field is a continuum in space into the water side of the interface, the angle of incidence in TIRF microscopes is often set to allow much of the intensity in the evanescent field to be limited to the first approximately 100 nm beyond the coverslip/slide surface. This is defined as the depth of penetration of the field or the axial distance over which the intensity drops off by a factor of e . In reality, this depth of penetration can actually be adjusted over a wide range. 'Objective lens TIRF', which is the most commonly employed mode of TIRF operation currently, uses a single objective lens to steer the incident beam and collect fluorescence emissions. Here, the depth of penetration can be set to be as small as approximately 30 nm for very high NA objective lens (e.g. NA = 1.65) or can be made arbitrarily larger (extending in principle to infinity).

TIRF in effect delimits the excitation field to result in selective illumination and excitation of fluorophores that are positioned close to the coverslip/slide surface (in practice, this 'close distance' can be approximated as being, very roughly, the depth of penetration itself). Thus, TIRF is particularly valuable for identifying single fluorescently labelled molecules integrated into cell membranes, for cells immobilized on to a glass slide/coverslip. Due to the fact that TIRF detects only minimal signals from the out-of-focus regions, the signal-to-noise ratio is significantly

improved, enabling better contrast for detecting single molecules [88]. In life science research, TIRF is often used in studies of kinetic properties on a single-molecule level in cell membranes, which is of particular importance in cellular signalling and vesicle trafficking research. For example, using TIRF microscopy the dynamics of the entire cascade of lipopolysaccharide transfer on to toll-like 4 receptor/myeloid differentiation factor 2 was reconstructed [109]. Moreover, TIRF can also be used in single-molecule electrochemistry. Thus, the group of Bo Zhang discovered that mesoporous silica reduces the rate of diffusion of fluorogenic redox molecules, enabling observation of single redox events. The study was carried out on fluorescent resorufin allowing analysis of adsorption, desorption and redox events by TIRF molecules on transparent ITO electrodes coated with mesoporous silica [110].

TIRF is widely used in cytoskeleton assembly studies. Thus, TIRF provided novel insights into actin filament dynamics and network architecture on a single filament [111] as well as single-molecule detection sensitivity for the visualization and analysis of capping and uncapping of individual actin filaments in vertebrates [112]. Single-molecule TIRF revealed that, depending on the filament age, trafficking of myosin molecules results in sorting to different F-actin networks [113]. Enabled/vasodilator-stimulated phosphoprotein (Ena/VASP) regulates actin network assembly by interacting with actin filaments. TIRF revealed multiple modes of VASP–F-actin interactions underlying mechanisms of VASP action [114]. A detailed application of TIRF and other single-molecule methods on actin assembly and disassembly have been described recently [115].

‘Near TIRF’ (also known as HILO or oblique-angle epifluorescence), enhances imaging contrast but enables greater depth of imaging for non-surface processes (Figure 2D). HILO techniques can therefore be very beneficial in single-molecule studies in live cells. Both HILO and TIRF can be used for visualization of molecular diffusion. For example, these techniques were applied in studies of the behaviour of CheY, a protein used by *Escherichia coli* in its chemotactic response, revealing movements among chemoreceptor clusters, flagellar motors and switch complexes [116]. Dynamic properties of the plasma membrane were described by single-molecule tracking visualized by TIRF. The mobility of some proteins in the plasma membrane was identified by the work of Kusumi et al. as being putatively confined hop diffusion which does not depend upon the extracellular matrix and extracellular domains of proteins [117]. Several years earlier, Kusumi et al. used the same approach to examine MHC class II protein diffusion [118].

TIRF imaging of a human serotonin transporter (SERT) was used to study its diffusion at the plasma membrane and endoplasmic reticulum (ER) revealing stable and highly mobile fractions of SERT at the ER [119]. Later, various oligomeric forms of SERT were identified. In the same study, a combination of TIRF with ‘thinning out clusters while conserving stoichiometry’ (TOCCSL) was used to determine the oligomeric states of the proteins in both the compartments. However, TOCCSL can be used for studies of the mobile protein fractions only [120].

Molecular transport based on kinesin and dynein movements along microtubule filaments is fundamental for various cellular processes such as mitosis, meiosis, proteins, mRNA and organelle cargos, which are crucial for survival and morphogenesis [121]. Significant mechanistic insights into kinesin-based transport, for example, were obtained by single-molecule TIRF imaging of single GFP-labelled kinesins [122].

FRET

FRET is one of the most commonly used techniques to study putative interactions between neighbouring molecules. FRET utilizes the principle of non-radiative energy transfer between a donor and an acceptor molecule, which are often, but not exclusively, fluorescent (Figure 3A). If these molecules are close enough, typically separated by less than approximately 10 nm, then a donor being in an excited electronic state can transfer its excitation energy to an acceptor through electronic resonance of molecular orbitals [123,124]. This technique is commonly used in the study of a range of molecular interactions, in particular protein–protein and protein–nucleic acid. Temperature-dependent conformational changes of proteins, protein folding on a millisecond range, as well as dynamics of intrinsically disordered proteins, are possible to determine by combining FRET with a confocal microscopy excitation mode [125]. For example, confocal single-molecule FRET was used for determination of conformational changes in the *Listeria monocytogenes* P-type ATPase, LMC1, during its functional cycle [126].

Application of single-molecule FRET has been used in a range of protein-based molecular motors which act on DNA. One recent example of this is the replicative DNA helicase. Bell et al. from Howard Hughes Medical Institute, monitored opening and closing of *S. cerevisiae* ring-shaped Mcm2–7 DNA helicases during recruitment of the pre-replicative complex to the origin of replication. These observations provided novel insights into the mechanism of replication initiation and quality control [127]. FRET studies on chicken Werner syndrome ATP-dependent helicase (WRN helicase) revealed a mechanism of DNA unwinding by WRN. Thus, this helicase unwinds DNA in a repetitive manner: repetitive DNA unwinding by WRN which happens on forked, 3′/5′-overhanging, G4 containing DNA substrates, although results of this phenomenon do depend on a DNA substrate [128]. Single-molecule FRET has been

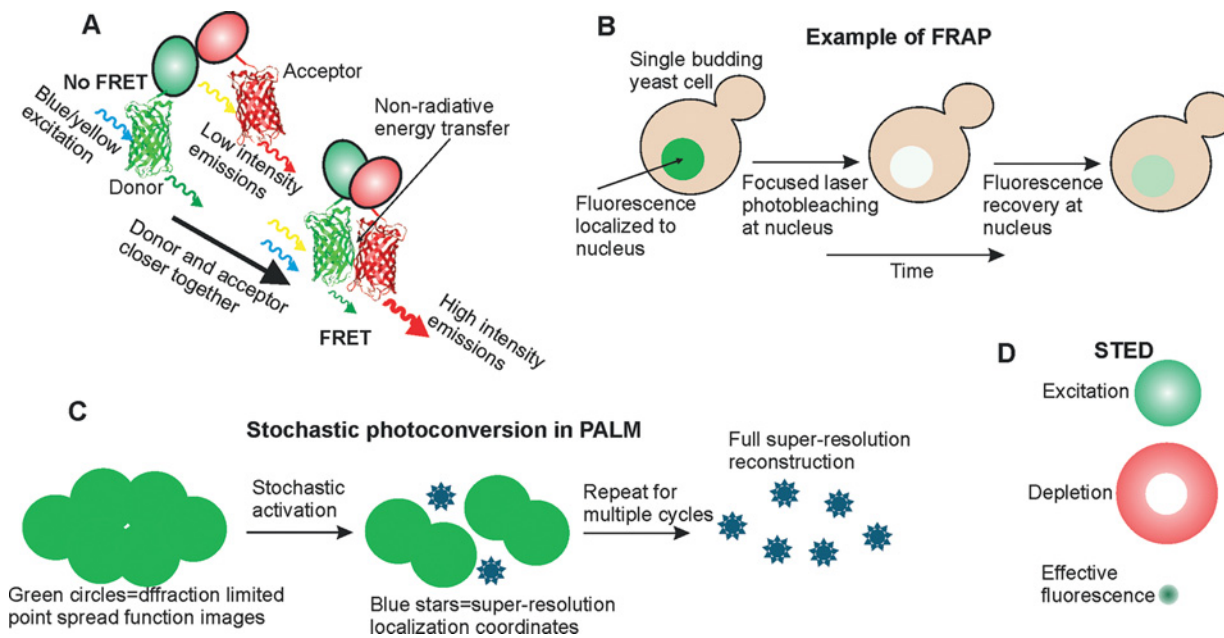


Figure 3. Examples of methods used in single-molecule studies

(A) **FRET principle** based on the non-radiative energy transfer which occurs when donor and acceptor dye pairs (often, but not exclusively, fluorophores) are positioned within typically less than approximately 10 nm of each other (explanation is provided in the text); (B) **FRAP** illustrating photobleaching of fluorophores in a delimited region of a biological sample, here shown with a single budding yeast cell in which fluorescently labelled material in the nucleus is photobleached, followed by the measurement of fluorescence recovery over time; (C) **SMLM techniques (here exemplified with PALM)** illustrating selective activation of fluorophores and the final image after multiple photoactivation cycle repeats; and (D) **STED** showing excitation and depletion laser beams, and the effective fluorescence profile following stimulated depletion. Abbreviations: PALM, photoactivated localization microscopy; SMLM, single molecule localization microscopy; STED, stimulated emission depletion.

actively used in studies of DNA origami to obtain information about molecular structure and dynamics [129]. An energy transfer on a DNA origami substrate was visualized by using four-coloured FRET [130].

FRET-based biosensors have been only very recently developed but have rapidly become a widely used tool in the study of protein dynamics. One of the applications is the use of FRET-based sensors for determination and quantification of biomolecular crowding in live cells as an indicator of the physicochemical state of the cytoplasm [131]. Mechanical tension FRET sensors can also be used to study extra- and intracellular single-molecule force measurements [132]. DNA FRET sensors combined with TIRF imaging have been used to monitor DNA synthesis in real time where a simple setup utilizes a DNA primer labelled with a fluorophore acceptor and annealed to the DNA template which is labelled with the donor fluorophore. Molecular conformational changes upon extension altered the FRET signal which acted as a metric for DNA synthesis [133].

Significant recent progress has been achieved in studies of amyloid assembly processes by using single-molecule FRET combined with pulsed interleaved excitation (PIE) and fluorescence lifetime imaging microscopy (FLIM). Through reconstruction of the donor, FRET and acceptor images, as well as obtaining various parameters like FRET efficiency and fluorescence lifetimes, this technique enables the dynamics of protein aggregation to be followed. Thus, a two-step nucleation mechanism for amyloid fibrils formation through oligomerization was revealed [134].

FRAP

FRAP involves in essence photobleaching a region of a cell or tissue in which a specific fluorescently labelled component is localized, and then quantifying the extent of any recovery of fluorescence intensity in that region subsequently (Figure 3B). Since unbleached components from outside this bleached area would have had to diffuse back into this area, such fluorescence intensity recovery is a metric of molecular mobility and turnover processes. The pioneering development of FRAP emerged from Watt Webb's lab in the 1970s [135]. FRAP is now an established tool for enabling identification of molecular transport parameters such as diffusion and velocity coefficients, as well as kinetic parameters where molecular binding and unbinding events are involved [135]. For example, the localizations of nuclear

envelope transmembrane (NET) proteins and their translocation rates on the inner and outer nuclear membranes were resolved by applying single-point illumination single-molecule FRAP [136]. FRAP analysis was used to determine diffusion coefficients of stromal interaction protein 1 (STIM1), a calcium sensor and a selective ion channel Orai1 at ER–plasma membrane junctions, revealing the dynamics of STIM1–Orai1 interactions [137].

Binding dynamics were also determined for protein–DNA and protein–protein interactions, for example glucocorticoid and mineralocorticoid receptors binding to DNA [138] and interaction dynamics between STAT2 and USP18 participating in type I interferon signalling [139] respectively. FRAP is also one of the main techniques to study anisotropic molecular diffusion on a less than micrometre length scale. Similarly, FRAP and single-molecule tracking visualized by wide-field fluorescence microscopy can be used in diffusion measurements and microdomain structure identification of a cylinder-forming polystyrene-poly(ethylene oxide) diblock copolymer (PS-*b*-PEO) film [140].

PALM/STORM

Photoactivated localization microscopy (PALM) and stochastic optical reconstruction microscopy (STORM) are far-field imaging approaches that detect fluorescence following a photoconversion process of the fluorophore, either photoactivation in the case of PALM or photoswitching in the case of STORM. PALM/STORM techniques are examples of single molecule localization microscopy (SMLM), though, as discussed in the section above on the key historical developments, localization microscopy can be applied to single fluorescent molecules without requiring a photoconversion process. Additionally, the critical difference between PALM and STORM is not the type of fluorophore as such but rather the sequenced compared with random activation. In most PALM applications, fluorophores are stochastically activated and then imaged, activated then imaged etc. in multiple cycles (Figure 3C). In most STORM applications, the activation and imaging happen simultaneously, which can significantly increase the rate of data collection. PALM type imaging is also extremely useful in single-particle tracking type approaches. One or a very small number of fluorophores are excited at a given time, thus, their diffraction-limited areas do not overlap (Figure 3C). Excitation cycles can be repeated until all locations of target molecules are detected, which then can be assembled into the final image [141–143]. Therefore, PALM and STORM provide a wide range of applications in various fields of studies. These types of SMLM techniques have been widely used in recent cancer research. Yiping Ciu's group applied these methods in order to visualize and track exosomes in human breast and cervical cancer cells (SKBR3 and HeLa cell lines respectively). By applying indirect immunofluorescence labelling with organic dyes, e.g. Alexa Fluor 488 and Alexa Fluor 647, the group showed accumulation of exosomes in lysosomes as well as interactions of cancer-derived exosomes with normal cells [144].

Plasma membrane research also benefits from using SMLM methods. For example, STORM allows dynamic tracking of N- and O-linked glycans on the membrane of live mammary cancer cells [145]. PALM was applied in the studies of protein organization in the plasma membrane, in particular, organization of glycosylphosphatidylinositol-linked proteins [146]. This technique is also extensively used in studies of protein oligomerization. For example, PALM revealed a multimeric organization of the Raf serine/threonine kinase which regulates cell growth through MAPK cascades [147]. Single molecules of G-protein-coupled receptor which become organized into dimers and higher oligomers were also visualized by PALM [148]. PhotoGate is an alternative to the PALM technique, which uses the principle of photobleaching of fluorescent particles and controls the number of fluorophores that enter the region of interest. Fluorescent particles that arrive at the region of interest are repeatedly photobleached, thus, the concentration of fluorophores in the region of interest remains constant. Hence, PhotoGate does not require the use of photoconvertible fluorescent proteins but allows longer time for tracking single particles tagged with traditional fluorescent proteins (eGFP, mNeonGreen). Thus, this method enabled observation of monomer–dimer transitions of EGF receptor on a cell membrane as well as its intracellular signalling mediator, APPL1, interactions with early endosomes [149].

Combinations of PALM with other techniques allow studies of protein–protein interaction on a nanoscale level. A valuable method for probing protein–protein interactions is biomolecular fluorescence complementation (BiFC). In BiFC, one of the interacting proteins is labelled with a truncated version of a fluorescent protein, which is not fluorescent. A putative interacting protein can be labelled with the remaining truncated part of the fluorescent protein which similarly on its own is not fluorescent. If the two proteins interact the two complementary parts of the fluorescent protein can bind together, thus, an intact fluorescent protein molecule is restored which may then be excited into fluorescence [150]. However, the intrinsic spatial resolution of the technique is still limited by the diffraction of light [151]. Therefore, simultaneous use of BiFC and a super-resolution technique like PALM can enable imaging with, at best, approximately nanometre spatial precision. For instance, BiFC-PALM in studies of Ras GTPase and interactions with its downstream effector Raf showed Ras/Raf complexes assembling on the cellular membrane [151].

A year later, the same group showed a novel mechanism involved in cell signalling where signal transduction through MAPK pathways activation is dependent on Ras–GTP dimerization [152].

PALM has been used in biomineralization studies to investigate roles of biosilica-associated proteins in biosilica morphogenesis. Photoconvertible fluorescent proteins, Dendra2, mEos3.2 and Dronpa, were fused to biosilica-associated protein Silaffin-3 of model diatom *Thalassiosira pseudonana* [153].

Further development of SMLM methods has transformed them into techniques capable of obtaining multidimensional data. 3D information provides important insight into the architecture of molecules and systems, shedding new light on their structure and organization. For the first time, 3D PALM was used to visualize plasma membranes and integrin receptors within the ER [154]. Multicolour 3D STORM revealed molecular architectures of synapses in the brain, variations in their morphology, distribution and composition of neurotransmitter receptor [155]. Multidimensional imaging was applied to the studies of the cytoskeleton. For example, 3D PALM observations of live *Caulobacter crescentus* bacteria revealed organizations of a tubulin-like cytoskeletal protein FtsZ, providing direct evidence of its arrangement into Z-ring upon cell division [156]. 3D STORM using inclined illumination astigmatism imaging was employed in attempt to better understand the organization of F-actin [157]. 3D PALM has also been used in chromatin studies, for example to follow the distribution of the H2B histone, one of the core histones that form the nucleosome [158], and for imaging a budding yeast specialized H3 histone, Cse4 [159].

STED

STED microscopy method, as discussed earlier, was experimentally demonstrated first by Stefan Hell, reported in 1994. This far-field method breaks down the diffraction limit through minimizing the area of excitation at the focal waist by controlled selective de-excitation of a target fluorophore. The focal plane is scanned by two laser beams (Figure 3D). The first one excites the fluorophores, the second beam of a longer wavelength is specifically altered such that at the focal plane has a donut shape. Therefore, only a small area from the centre of the donut shape is left to be able to emit the light. Thus the STED technique enables imaging below the diffraction limit [61,160].

Dual-channel STED for the first time allowed identification and characterization of signalling pathways involving astrocyte $\alpha\text{v}\beta\text{3}$ integrin and neuronal Thy-1 receptor, a cell adhesion molecule which is constantly expressed in the central nervous system. The capacity of STED to resolve Thy-1 clusters, with an effective diameter of 40–50 nm, revealed the involvement of this protein in the neuronal actin skeleton alterations [161]. A potential new role of the neuronal apoptosis inhibitory protein (NAIP), one of the proteins investigated in neurodegenerative disorders, was suggested after STED imaging of NAIP cellular localization upon cytokinesis [162].

STED microscopy can be also applied in various studies of the nucleus, such as chromatin studies via visualizing chromatin structure and characterization of architectural rearrangement invoked by physiological stimuli [163], looking at the spatial distribution of dsDNA repair factors [164] and replication factories [165], nuclear pore complex investigations via determination of NUP62 and NUP214 distributions [166].

There are a number of variants of STED approaches which all comprise light-induced transitions between at least two molecular states (e.g. bright and dark), one of which is fluorescent. A biologically valuable example of one of these STED variants is called reversible saturable/switchable optical fluorescence transition (RESOLFT), which stands for reversible saturable/switchable optical (fluorescence) transitions [167]. Like STED, the RESOLFT resolution goes beyond the diffraction limit, hence, allows nanoscale precise microscopy studies. Recent applications of RESOLFT using reversibly switchable fluorescent proteins have enabled visualization of individual spines within living hippocampal brain tissue [168], vimentin filaments [169], keratin and a structural protein of the nuclear pore complex [170]. Another variant of STED, MINFLUX, which like PALM/STORM uses selective stochastic fluorophore switching on and off, has been developed recently. MINFLUX allows 1 nm precision of molecules located 6 nm apart. This technique was used to image DNA origami and demonstrate diffusion of 30S ribosome subunit in *E. coli* [171].

3D single-molecule fluorescence microscopy tools

Another super-resolution method includes structured illumination microscopy (SIM). SIM illuminates the sample with a spatially periodic, structured illumination pattern, typically a series of grid-like patterns illuminated in different acquisitions at different orientations relative to the sample. The image is then analysed in so-called Fourier or frequency space. Small features in ‘real’ space have high spatial frequency values in Fourier space. Normal optical microscopy is limited by the optical resolution at the highest spatial frequency value that can be resolved in Fourier space, however, the periodic features of the structured illumination pattern can interfere with the high spatial frequency components in the sample to produce a ‘beat’ signal in Fourier space, due to the so-called Moiré effect, whose absolute value is lower than the threshold upper limit set by the optical resolution limit. Therefore, this beat signal

contains super-resolution information which goes beyond the standard optical diffraction limit [172]. SIM improves the resolution of conventional light microscopy by a factor of roughly two in all three (x , y and z) spatial dimensions, which makes it a powerful tool in various fields of studies, such as the morphology of erythrocytes [173], the 3D structures of liver fenestrations and sieve plates [174], and in discerning precise details of subdiffraction limit of cortical microtubules [175]. There are, however, still some issues with SIM in that the structured illumination pattern can also result in the appearance of artifacts on the image of the orientation and spacing of the illumination grid used, despite image analysis algorithms which are applied to attempt to remove these subsequently.

Some of the recent 3D fluorescence imaging methods, including double-helix microscopy developed by the group of Moerner et al. [176], and astigmatism can be implemented as an addition to many currently developed fluorescence microscopes as the required equipment can often be placed between the objective lens and the camera with relatively minor expertise in optical alignment required [61]. For instance, single-molecule localization microscopy in combination with astigmatism imaging applied to formalin-fixed, paraffin-embedded (FFPE) breast cancer samples after immunostaining, has enabled the visualization of proteins in mitochondrial and nuclear membranes as well as a cellular membrane protein (oestrogen receptor Her2) which is overexpressed in one-fourth of the cells [177]. RNA polymerase movements along DNA during the transcription cycle were tracked using 3D super-resolution imaging [178]. 3D single-molecule localization microscopy and 3D STORM are used in imaging fixed brain tissues allowing identification of several proteins simultaneously [179]. Also, a novel technique entitled cryogenic optical localization (COLD) has been reported recently. COLD provides spatial information about molecules through resolving 3D positions of several fluorophores attached to a single protein [180]. Detailed description of 3D super-resolution single-molecule microscopy methods has been published recently [181], and we steer the reader to this review for more detailed information.

There have been other attempts to improve existing 2D techniques in order to obtain higher spatial dimension resolution. For example, lattice light-sheet (LLS) microscopy has been successfully used as a non-invasive 4D imaging technique (three spatial dimensions plus the dimension of time) of live cells which allows visualization of intracellular dynamics [182]. LLS microscopy has also been combined with point accumulation for imaging of nanoscale topography (PAINT) microscopy [183]. In PAINT, the sample is continuously targeted by fluorescent probes present in solution throughout the imaging process [184]. LLS-PAINT with various PAINT labels enables 3D multicolour imaging of DNA and intracellular membranes during cell division [183]. Other variants of PAINT, such as DNA-PAINT and Exchange-PAINT, enable 2D and 3D visualization of DNA nanostructures as well as kinetic studies of DNA binding using a single fluorescent dye [185,186].

Future perspectives

Extensive use of single-molecule fluorescence microscopy techniques have enabled visualization of an enormous range of different biological processes which was previously restricted by traditional population ensemble average methods. Many of the biological processes studied are components of very basic and fundamental systems in the cell. However, they have been essentially invisible until now: long-standing 'old' problems that have been simply intractable until the arrival of modern single-molecule fluorescence microscopy methods. The new tools have provided novel insights into the basic mechanisms of live cells as well as the identification of previously unknown functions of molecules which are essential to life as we know it. Despite recent achievements in making the invisible visible, experimental limitations do remain. For example, the signal-to-noise ratio can still be improved, especially when very rapid imaging is required to address biological questions at the submillisecond time scale. There is still a need for novel fluorescent proteins with enhanced brightness and photostability which would increase the possible illumination times and thus enable longer observations of molecules and processes in which they partake. Similarly, fluorescent proteins significantly increase the overall size of the tagged protein construct, since a fluorescent protein is often of comparable molecular weight with the native protein itself, which might affect its natural molecular conformations and thus its physiological behaviour and function. Therefore, the next generation of fluorescent molecules we would hope might become much smaller in size or even disappear completely.

For example, attempts to use digital holography as a super-resolution microscopy technique have already been made [187,188], with label-free imaging rendering, for example promising structural details of the dynamic morphology of filaments which enable single swimming cells to be motile [189]. Another example of a label-free technique is an interferometric scattering microscopy (iSCAT) with a single-molecule precision, applied recently to a range of biological questions by the group of Kukura et al. [190,191]. iSCAT has now been used in studies of motor proteins dynamics [192] which enabled visualization of microtubule disassembly [193], uncovered unknown details of myosin-5 stepping mechanism [194], and provided novel insights into kinesin-1 stepping cycle [195].

At present, there is no unique, single technique which can enable the simultaneous visualization of proteins and their post-translational modifications, for example as occurs during signal transduction. It would, in principle, also be valuable if we were able to obtain data concerning the molecular conformational states of intrinsically disordered regions during protein–protein or protein–nucleic acid interactions. However, attempts to study molecular conformational changes upon mechanical stretching perturbations have already been made by combining single-molecule fluorescence microscopy techniques with non-fluorescence approaches. For example, Fernandez et al. have utilized TIRF and AFM simultaneously to study the dynamics of stretching and unfolding of ubiquitin protein domains [196]. Combinations of AFM and FRET were also applied in studies of HPPK (6-hydroxymethyl-7,8-dihydropterin pyrophosphokinase) conformation [197]. TIRF and AFM-based single-cell force spectroscopy were also used in non-mechanistic studies and revealed protein cluster formation of integrins and their recruitment of adhesion protein [198].

There is no doubt that scientific excellence in the development of novel biophysical tools and techniques will continue to push back the borders of our understanding of life's complex processes much further than at present. Interdisciplinary science approaches, when appropriately funded, are the best way forward to achieve these new developments.

Competing interests

The authors declare that there are no competing interests associated with the manuscript.

Funding

This work was supported by the Royal Society Newton International Fellowship [grant number NF160208] and the BBSRC [grant number BB/N006453/1].

Abbreviations

BiFC, biomolecular fluorescence complementation; CLSM, confocal laser scanning microscopy; COLD, cryogenic optical localization; EGF, epidermal growth factor; ER, endoplasmic reticulum; HILO, highly inclined and laminated optical sheet; iRFP, IR fluorescent protein; iSCAT, interferometric scattering microscopy; LLS, lattice light-sheet; PAINT, point accumulation for imaging of nanoscale topography; PALM, photoactivated localization microscopy; RESOLFT, reversible saturable/switchable optical fluorescence transition; SERT, serotonin transporter; SIM, structured illumination microscopy; SMLM, single molecule localization microscopy; STED, stimulated emission depletion; STIM1, stromal interaction protein 1; STORM, stochastic optical reconstruction microscopy; TIRF, total internal reflection fluorescence; TOCCSL, thinning out clusters while conserving stoichiometry; WRN helicase, Werner syndrome ATP-dependent helicase.

References

- 1 Elsassser, W.M. (1984) Outline of a theory of cellular heterogeneity (cell biology/theoretical biology). *Cell Biol.* **81**, 5126–5129
- 2 Rubin, H. (1990) The significance of biological heterogeneity. *Cancer Metastasis Rev.* **9**, 1–20
- 3 (2010) Hunting down heterogeneity. *Nat. Chem. Biol.* **6**, 691
- 4 Sott, K., Eriksson, E., Petelenz, E. and Goksör, M. (2008) Optical systems for single cell analyses. *Expert Opin. Drug Discov.* **3**, 1323–1344
- 5 Leake, M.C. (2013) *Single-Molecule Cellular Biophysics*, Cambridge University Press
- 6 Perkel, J.M. (2015) Single-cell biology: the power of one. *Science* **350**, 696–698
- 7 Leake, M.C. (2010) Shining the spotlight on functional molecular complexes: the new science of single-molecule cell biology. *Commun. Integr. Biol.* **3**, 415–418
- 8 Harriman, O.L.J. and Leake, M.C. (2011) Single molecule experimentation in biological physics: exploring the living component of soft condensed matter one molecule at a time. *J. Phys. Condens. Matter* **23**, 503101
- 9 Elowitz, M.B., Levine, A.J., Siggia, E.D. and Swain, P.S. (2002) Stochastic gene expression in a single cell. *Science* **297**, 1183–1186
- 10 Chiu, S.-W. and Leake, M.C. (2011) Functioning nanomachines seen in real-time in living bacteria using single-molecule and super-resolution fluorescence imaging. *Int. J. Mol. Sci.* **12**, 2518–2542
- 11 Leake, M.C. (2012) The physics of life: one molecule at a time. *Philos. Trans. R. Soc. London B. Biol. Sci.* **368**, 20120248
- 12 Lenn, T. and Leake, M.C. (2012) Experimental approaches for addressing fundamental biological questions in living, functioning cells with single molecule precision. *Open Biol.* **2**, 120090
- 13 Shashkova, S., Wollman, A.J., Leake, M.C. and Hohmann, S. (2017) The yeast Mig1 transcriptional repressor is dephosphorylated by glucose-dependent and independent mechanisms. *FEMS Microbiol. Lett.*, doi:10.1093/femsle/fnx133
- 14 Xue, Q., Harriman, O. and Leake, M.C. (2011) Using bespoke fluorescence microscopy to study the soft condensed matter of living cells at the single molecule level. *J. Phys. Conf. Ser.* **286**, 12001
- 15 Leake, M.C. (2016) *Biophysics: Tools and Techniques*, CRC Press
- 16 Lu, H.P., Xun, L. and Xie, X.S. (1998) Single-molecule enzymatic dynamics. *Science* **282**, 1877–1882

- 17 Sowa, Y., Rowe, A.D., Leake, M.C., Yakushi, T., Homma, M., Ishijima, A. et al. (2005) Direct observation of steps in rotation of the bacterial flagellar motor. *Nature* **437**, 916–919
- 18 Leake, M.C., Chandler, J.H., Wadhams, G.H., Bai, F., Berry, R.M. and Armitage, J.P. (2006) Stoichiometry and turnover in single, functioning membrane protein complexes. *Nature* **443**, 355–358
- 19 Reid, S.W., Leake, M.C., Chandler, J.H., Lo, C.-J., Armitage, J.P. and Berry, R.M. (2006) The maximum number of torque-generating units in the flagellar motor of *Escherichia coli* is at least 11. *Proc. Natl. Acad. Sci. U.S.A.* **103**, 8066–8071
- 20 Delalez, N.J., Wadhams, G.H., Rosser, G., Xue, Q., Brown, M.T., Dobbie, I.M. et al. (2010) Signal-dependent turnover of the bacterial flagellar switch protein FliM. *Proc. Natl. Acad. Sci. U.S.A.* **107**, 11347–11351
- 21 Rowe, A.D., Leake, M.C., Morgan, H. and Berry, R.M. (2003) Rapid rotation of micron and submicron dielectric particles measured using optical tweezers. *J. Mod. Opt.* **50**, 1539–1554
- 22 Leake, M.C., Greene, N.P., Godun, R.M., Granjon, T., Buchanan, G., Chen, S. et al. (2008) Variable stoichiometry of the TatA component of the twin-arginine protein transport system observed by *in vivo* single-molecule imaging. *Proc. Natl. Acad. Sci. U.S.A.* **105**, 15376–15381
- 23 Deniz, A.A., Mukhopadhyay, S. and Lemke, E.A. (2008) Single-molecule biophysics: at the interface of biology, physics and chemistry. *J. R. Soc. Interface* **5**, 15–45
- 24 Bryan, S.J., Burroughs, N.J., Shevela, D., Yu, J., Rupprecht, E., Liu, L.-N. et al. (2014) Localisation and interactions of the Vipp1 protein in cyanobacteria. *Mol. Microbiol.* **94**, 1179–1195
- 25 Nenninger, A., Mastroianni, G., Robson, A., Lenn, T., Xue, Q., Leake, M.C. et al. (2014) Independent mobility of proteins and lipids in the plasma membrane of *Escherichia coli*. *Mol. Microbiol.* **92**, 1142–1153
- 26 Wollman, A.J.M. and Leake, M.C. (2016) Single molecule narrowfield microscopy of protein-DNA binding dynamics in glucose signal transduction of live yeast cells. *Methods Mol. Biol.* **1431**, 5–15
- 27 Leake, M.C., Wilson, D., Bullard, B. and Simmons, R.M. (2003) The elasticity of single kettin molecules using a two-bead laser-tweezers assay. *FEBS Lett.* **535**, 55–60
- 28 Leake, M.C., Wilson, D., Gautel, M. and Simmons, R.M. (2004) The elasticity of single titin molecules using a two-bead optical tweezers assay. *Biophys. J.* **87**, 1112–1135
- 29 Linke, W.A. and Leake, M.C. (2004) Multiple sources of passive stress relaxation in muscle fibres. *Phys. Med. Biol.* **49**, 3613–3627
- 30 Leake, M.C., Grütznér, A., Krüger, M. and Linke, W.A. (2006) Mechanical properties of cardiac titin's N2B-region by single-molecule atomic force spectroscopy. *J. Struct. Biol.* **155**, 263–272
- 31 Bullard, B., Garcia, T., Benes, V., Leake, M.C., Linke, W.A. and Oberhauser, A.F. (2006) The molecular elasticity of the insect flight muscle proteins projectin and kettin. *Proc. Natl. Acad. Sci. U.S.A.* **103**, 4451–4456
- 32 Zhou, Z., Miller, H., Wollman, A. and Leake, M. (2015) Developing a new biophysical tool to combine magneto-optical tweezers with super-resolution fluorescence microscopy. *Photonics* **2**, 758–772
- 33 Reyes-Lamothe, R., Sherratt, D.J. and Leake, M.C. (2010) Stoichiometry and architecture of active DNA replication machinery in *Escherichia coli*. *Science* **328**, 498–501
- 34 Badrinarayanan, A., Reyes-Lamothe, R., Uphoff, S., Leake, M.C. and Sherratt, D.J. (2012) *In vivo* architecture and action of bacterial structural maintenance of chromosome proteins. *Science* **338**, 528–531
- 35 Beattie, T.R., Kapadia, N., Nicolas, E., Uphoff, S., Wollman, A.J., Leake, M.C. et al. (2017) Frequent exchange of the DNA polymerase during bacterial chromosome replication. *Elife* **6**, e21763
- 36 Wollman, A.J.M., Miller, H., Zhou, Z. and Leake, M.C. (2015) Probing DNA interactions with proteins using a single-molecule toolbox: inside the cell, in a test tube and in a computer. *Biochem. Soc. Trans.* **43**, 139–145
- 37 Badrinarayanan, A. and Leake, M.C. (2016) Using fluorescence recovery after photobleaching (frap) to study dynamics of the structural maintenance of chromosome (SMC) complex *in vivo*. *Methods Mol. Biol.* **1431**, 37–46
- 38 Lenn, T., Leake, M.C. and Mullineaux, C.W. (2008) Clustering and dynamics of cytochrome bd-I complexes in the *Escherichia coli* plasma membrane *in vivo*. *Mol. Microbiol.* **70**, 1397–1407
- 39 Lenn, Y.T., Leake, M.C. and Mullineaux, C.W. (2008) Are *Escherichia coli* OXPHOS complexes concentrated in specialized zones within the plasma membrane. *Biochem. Soc. Trans.* **36**, 1032–1036
- 40 Lenn, T. and Leake, M.C. (2016) Single-molecule studies of the dynamics and interactions of bacterial OXPHOS complexes. *Biochim. Biophys. Acta* **1857**, 224–231
- 41 Llorente-García, I., Lenn, T., Erhardt, H., Harriman, O.L., Liu, L.-N., Robson, A. et al. (2014) Single-molecule *in vivo* imaging of bacterial respiratory complexes indicates delocalized oxidative phosphorylation. *Biochim. Biophys. Acta* **1837**, 811–824
- 42 Miller, H., Wollman, A.J.M. and Leake, M.C. (2016) Designing a single-molecule biophysics tool for characterizing DNA damage for techniques that kill infectious pathogens through DNA damage effects. *Adv. Exp. Med. Biol.* **915**, 115–127
- 43 Wollman, A.J.M., Syeda, A.H., McGlynn, P. and Leake, M.C. (2016) Single-molecule observation of DNA replication repair pathways in *E. coli*. *Adv. Exp. Med. Biol.* **915**, 5–16
- 44 Zhou, Z. and Leake, M.C. (2016) Force spectroscopy in studying infection. *Adv. Exp. Med. Biol.* **915**, 307–327
- 45 Biteen, J.S., Thompson, M.A., Tselentis, N.K., Bowman, G.R., Shapiro, L. and Moerner, W.E. (2008) Super-resolution imaging in live *Caulobacter crescentus* cells using photoswitchable EYFP. *Nat. Methods* **5**, 947–949
- 46 Kuzmenko, A., Tankov, S., English, B.P., Tarassov, I., Tenson, T., Kamenski, P. et al. (2011) Single molecule tracking fluorescence microscopy in mitochondria reveals highly dynamic but confined movement of Tom40. *Sci. Rep.* **1**, 195
- 47 Padilla-Parra, S., Matos, P.M., Kondo, N., Marin, M., Santos, N.C. and Melikyan, G.B. (2012) Quantitative imaging of endosome acidification and single retrovirus fusion with distinct pools of early endosomes. *Proc. Natl. Acad. Sci. U.S.A.* **109**, 17627–17632

- 48 Liu, S.-L., Zhang, Z.-L., Sun, E.-Z., Peng, J., Xie, M., Tian, Z.-Q. et al. (2011) Visualizing the endocytic and exocytic processes of wheat germ agglutinin by quantum dot-based single-particle tracking. *Biomaterials* **32**, 7616–7624
- 49 Crane, J.M., Van Hoek, A.N., Skach, W.R. and Verkman, A.S. (2008) Aquaporin-4 dynamics in orthogonal arrays in live cells visualized by quantum dot single particle tracking. *Mol. Biol. Cell* **19**, 3369–3378
- 50 Bisson-Filho, A.W., Hsu, Y.-P., Squyres, G.R., Kuru, E., Wu, F., Jukes, C. et al. (2017) Treadmilling by FtsZ filaments drives peptidoglycan synthesis and bacterial cell division. *Science* **355**, 739–743
- 51 van Loenhout, M.T.J., de Grunt, M.V. and Dekker, C. (2012) Dynamics of DNA Supercoils. *Science* **338**, 94–97
- 52 Leake, M.C. (2014) Analytical tools for single-molecule fluorescence imaging in cellulose. *Phys. Chem. Chem. Phys.* **16**, 12635–12647
- 53 Xue, Q., Jones, N.S. and Leake, M.C. (2010) A general approach for segmenting elongated and stubby biological objects: extending a chord length transform with the radon transform. *2010 7th IEEE International Symposium on Biomedical Imaging: From Nano to Macro, ISBI 2010 - Proceedings* 161–164
- 54 Wollman, A.J.M., Miller, H., Foster, S. and Leake, M.C. (2016) An automated image analysis framework for segmentation and division plane detection of single live *Staphylococcus aureus* cells which can operate at millisecond sampling time scales using bespoke Slimfield microscopy. *Phys. Biol.* **13**, 05002
- 55 Xue, Q. and Leake, M.C. (2009) A novel multiple particle tracking algorithm for noisy *in vivo* data by minimal path optimization within the spatio-temporal volume. *Proceedings - 2009 IEEE International Symposium on Biomedical Imaging: From Nano to Macro, ISBI 2009* 1158–1161
- 56 Robson, A., Burrage, K. and Leake, M.C. (2013) Inferring diffusion in single live cells at the single-molecule level. *Philos. Trans. R. Soc. Lond. B Biol. Sci.* **368**, 20120029
- 57 Miller, H., Zhou, Z., Wollman, A.J.M. and Leake, M.C. (2015) Superresolution imaging of single DNA molecules using stochastic photoblinking of minor groove and intercalating dyes. *Methods* **88**, 81–88
- 58 Moerner, W.E. and Fromm, D.P. (2003) Methods of single-molecule fluorescence spectroscopy and microscopy. *Rev. Sci. Instrum.* **74**, 3597–3619
- 59 Jabłoński, A. (1933) Efficiency of anti-stokes fluorescence in dyes. *Nature* **131**, 839–840
- 60 Stokes, G.G., Trans, P. and Lond, R.S. (1852) On the change of refrangibility of light. *Philos. Trans. R. Soc. Lond.* **142**, 463–562
- 61 Wollman, A.J.M., Nudd, R., Hedlund, E.G. and Leake, M.C. (2015) From animaculum to single molecules: 300 years of the light microscope. *Open Biol.* **5**, 150019–150019
- 62 Zimmer, M. (2009) GFP: from jellyfish to the Nobel prize and beyond. *Chem. Soc. Rev.* **38**, 2823–2832
- 63 Shimomura, O., Johnson, F.H. and Saiga, Y. (1962) Extraction, purification and properties of aequorin, a bioluminescent protein from the luminous hydromedusa, *Aequorea*. *J. Cell Comp. Physiol.* **59**, 223–239
- 64 Heim, R., Prasher, D.C., Tsien, R.Y. and Kandel, E.R. (1994) Wavelength mutations and posttranslational autoxidation of green fluorescent protein (*Aequorea victoria*/blue fluorescent protein/*Escherichia coli*/imidazolidinone). *Proc. Natl. Acad. Sci. U.S.A.* **91**, 12501–12504
- 65 Heim, R., Cubitt, A.B. and Tsien, R.Y. (1995) Improved green fluorescence. *Nature* **373**, 663–664
- 66 Zacharias, D.A., Violin, J.D., Newton, A.C. and Tsien, R.Y. (2002) Partitioning of lipid-modified monomeric GFPs into membrane microdomains of live cells. *Science* **296**, 913–916
- 67 Lippincott-Schwartz, J. and Patterson, G.H. (2003) Development and use of fluorescent protein markers in living cells. *Science* **300**, 87–91
- 68 Wiedenmann, J., Ivanchenko, S., Oswald, F., Schmitt, F., Röcker, C., Salihi, A. et al. (2004) EosFP, a fluorescent marker protein with UV-inducible green-to-red fluorescence conversion. *Proc. Natl. Acad. Sci. U.S.A.* **101**, 15905–15910
- 69 Chudakov, D.M., Lukyanov, S. and Lukyanov, K.A. (2007) Tracking intracellular protein movements using photoswitchable fluorescent proteins PS-CFP2 and Dendra2. *Nat. Protoc.* **2**, 2024–2032
- 70 Tsutsui, H., Karasawa, S., Shimizu, H., Nukina, N. and Miyawaki, A. (2005) Semi-rational engineering of a coral fluorescent protein into an efficient highlighter. *EMBO Rep.* **6**, 233–238
- 71 Ando, R., Hama, H., Yamamoto-Hino, M., Mizuno, H. and Miyawaki, A. (2002) An optical marker based on the UV-induced green-to-red photoconversion of a fluorescent protein. *Proc. Natl. Acad. Sci. U.S.A.* **99**, 12651–12656
- 72 Baker, S.M., Buckheit, III, R.W. and Falk, M.M. (2010) Green-to-red photoconvertible fluorescent proteins: tracking cell and protein dynamics on standard wide-field mercury arc-based microscopes. *BMC Cell Biol.* **11**, 15
- 73 Zhang, M., Chang, H., Zhang, Y., Yu, J., Wu, L., Ji, W. et al. (2012) Rational design of true monomeric and bright photoactivatable fluorescent proteins. *Nat. Methods* **9**, 727–729
- 74 Habuchi, S., Tsutsui, H., Kochaniak, A.B., Miyawaki, A. and van Oijen, A.M. (2008) mKikGR, a monomeric photoswitchable fluorescent protein. *PLoS ONE* **3**, e3944
- 75 McEvoy, A.L., Hoi, H., Bates, M., Platonova, E., Cranfill, P.J., Baird, M.A. et al. (2012) mMaple: a photoconvertible fluorescent protein for use in multiple imaging modalities. *PLoS ONE* **7**, e51314
- 76 Raarup, M.K., Fjorback, A.W., Jensen, S.M.R., Müller, H.K., Kjaergaard, M.M., Poulsen, H. et al. (2009) Enhanced yellow fluorescent protein photoconversion to a cyan fluorescent protein-like species is sensitive to thermal and diffusion conditions. *J. Biomed. Opt.* **14**, 034039
- 77 Kremers, G.-J., Hazelwood, K.L., Murphy, C.S., Davidson, M.W. and Piston, D.W. (2009) Photoconversion in orange and red fluorescent proteins. *Nat. Methods* **6**, 355–358
- 78 Nowotschin, S. and Hadjantonakis, A.-K. (2009) Use of KikGR a photoconvertible green-to-red fluorescent protein for cell labeling and lineage analysis in ES cells and mouse embryos. *BMC Dev. Biol.* **9**, 49
- 79 Filonov, G.S., Piatkevich, K.D., Ting, L.-M., Zhang, J., Kim, K. and Verkhusha, V.V. (2011) Bright and stable near-infrared fluorescent protein for *in vivo* imaging. *Nat. Biotechnol.* **29**, 757–761
- 80 Subach F, V., Subach, O.M., Gundorov, I.S., Morozova, K.S., Piatkevich, K.D., Cuervo, A.M. et al. (2009) Monomeric fluorescent timers that change color from blue to red report on cellular trafficking. *Nat. Chem. Biol.* **5**, 118–126

- 81 Keppler, A., Gendreizig, S., Gronemeyer, T., Pick, H., Vogel, H. and Johnsson, K. (2002) A general method for the covalent labeling of fusion proteins with small molecules *in vivo*. *Nat. Biotechnol.* **21**, 86–89
- 82 Los G, V., Encell, L.P., McDougall, M.G., Hartzell, D.D., Karassina, N., Zimprich, C. et al. (2008) HaloTag: a novel protein labeling technology for cell imaging and protein analysis. *ACS Chem. Biol.* **3**, 373–382
- 83 Turner, R.D., Hurd, A.F., Cadby, A., Hobbs, J.K. and Foster, S.J. (2013) Cell wall elongation mode in Gram-negative bacteria is determined by peptidoglycan architecture. *Nat. Commun.* **4**, 1496
- 84 Rotman, B. (1961) Measurement of activity of single molecules of beta-D-galactosidase. *Proc. Natl. Acad. Sci. U.S.A.* **47**, 1981–1991
- 85 Brooks Shera, E., Seitzinger, N.K., Davis, L.M., Keller, R.A. and Soper, S.A. (1990) Detection of single fluorescent molecules. *Chem. Phys. Lett.* **174**, 553–557
- 86 Abbe, E. (1873) Beitrage zur Theorie des Mikroskops und der mikroskopischen Wahrnehmung. *Arch. für. Mikroskopische Anat.* **9**, 413–420
- 87 Choquet, D. (2014) The 2014 Nobel Prize in Chemistry: a large-scale prize for achievements on the nanoscale The 2014 Nobel Prize in Chemistry awarded to. *Neuron* **84**, 1116–1119
- 88 Axelrod, D. (1981) Cell-substrate contacts illuminated by total internal reflection fluorescence. *J. Cell Biol.* **89**, 141–145
- 89 Funatsu, T., Harada, Y., Tokunaga, M., Saito, K. and Yanagida, T. (1995) Imaging of single fluorescent molecules and individual ATP turnovers by single myosin molecules in aqueous solution. *Nature* **374**, 555–559
- 90 Yanagida, T., Sako, Y. and Minoghchi, S. (2000) Single-molecule imaging of EGFR signalling on the surface of living cells. *Nat. Cell Biol.* **2**, 168–172
- 91 Betzig, E. and Chichester, R.J. (1993) Single molecules observed by near-field scanning optical microscopy. *Science* **262**, 1422–1425
- 92 Ha, T., Enderle, T., Ogletree, D.F., Chemla, D.S., Selvin, P.R. and Weiss, S. (1996) Probing the interaction between two single molecules: fluorescence resonance energy transfer between a single donor and a single acceptor. *Proc. Natl. Acad. Sci. U.S.A.* **93**, 6264–6268
- 93 Schmidt, T., Schutz, G.J., Baumgartner, W., Gruber, H.J. and Schindler, H. (1996) Imaging of single molecule diffusion (fluorescence microscopy/single dye detection/time-resolved imaging/quantal fluorescence/lipid bilayers). *Biophysics (Oxf.)* **93**, 2926–2929
- 94 Gelles, J., Schnapp, B.J. and Sheetz, M.P. (1988) Tracking kinesin-driven movements with nanometre-scale precision. *Nature* **331**, 450–453
- 95 Cox, S., Rosten, E., Monypenny, J., Jovanovic-Taliman, T., Burnette, D.T., Lippincott-Schwartz, J. et al. (2011) Bayesian localization microscopy reveals nanoscale podosome dynamics. *Nat. Methods* **9**, 195–200
- 96 Plank, M., Wadhams, G.H. and Leake, M.C. (2009) Millisecond timescale slimfield imaging and automated quantification of single fluorescent protein molecules for use in probing complex biological processes. *Integr. Biol. (Camb)* **1**, 602–612
- 97 Wollman, A.J.M. and Leake, M.C. (2015) Millisecond single-molecule localization microscopy combined with convolution analysis and automated image segmentation to determine protein concentrations in complexly structured, functional cells, one cell at a time. *Faraday Discuss.* **184**, 401–424
- 98 Thorley, J.A., Pike, J. and Rappoport, J.Z. (2014) Super-resolution microscopy: a comparison of commercially available options. *Fluorescence Microscopy: Super-Resolution and Other Novel Techniques*, pp. 199–212, Elsevier Inc
- 99 Okhonin, V.A. (1986) Method of investigating specimen microstructure. Patent SU 1374992.
- 100 Hell, S.W., Lindek, S., Cremer, C. and Stelzer, E.H.K. (1994) Confocal microscopy with an increased detection aperture: type-B 4Pi confocal microscopy. *Opt. Lett.* **19**, 222–224
- 101 Minsky, M. (1988) Memoir on inventing the confocal scanning microscope. *Scanning* **10**, 128–138
- 102 Marvin, M. (1961) Microscopy apparatus. Patent US3013467 A.
- 103 Egger, M.D. and Petran, M. (1967) New reflected-light microscope for viewing unstained brain and ganglion cells. *Science* **157**, 305–307
- 104 Semwogerere, D. and Weeks, E.R. (2008) Confocal microscopy. In *Encyclopedia of Biomaterials and Biomedical Engineering* (Wnek, G. and Bowlin, G., eds), pp. 705–714, CRC Press
- 105 Segers-Nolten, G.M.J., Wyman, C., Wijgers, N., Vermeulen, W., Lenferink, A.T.M., Hoeijmakers, J.H.J. et al. (2002) Scanning confocal fluorescence microscopy for single molecule analysis of nucleotide excision repair complexes. *Nucleic Acids Res.* **30**, 4720–4727
- 106 Lee, J., Miyanaga, Y., Ueda, M. and Hohng, S. (2012) Video-rate confocal microscopy for single-molecule imaging in live cells and superresolution fluorescence imaging. *Biophys. J.* **103**, 1691–1697
- 107 Tychinskii, V.P., Kufal', G.E., Vyshenskaya, T.V., Perevedentseva, E.V. and Nikandrov, S.L. (1997) Measurements of submicron structures with the Airyscan laser phase microscope. *Quantum Electron.* **27**, 735–739
- 108 Sivaguru, M., Urban, M.A., Fried, G., Wesseln, C.J., Mander, L. and Punyasena, S.W. (2016) Comparative performance of airyscan and structured illumination superresolution microscopy in the study of the surface texture and 3D shape of pollen. *Microsc. Res. Tech.*, doi:10.1002/jemt.22732
- 109 Kim, S.J. and Kim, H.M. (2017) Dynamic lipopolysaccharide transfer cascade to TLR4/MD2 complex via LBP and CD14. *BMB Rep.* **50**, 55–57
- 110 Lu, J., Fan, Y., Howard, M.D., Vaughan, J.C. and Zhang, B. (2017) Single-Molecule Electrochemistry on a Porous Silica-Coated Electrode. *J. Am. Chem. Soc.* **139**, 2964–2971
- 111 Hansen, S.D., Zuchero, J.B. and Mullins, R.D. (2013) Cytoplasmic actin: purification and single molecule assembly assays. *Methods Mol. Biol.* **1046**, 145–170
- 112 Kuhn, J.R. and Pollard, T.D. (2007) Single molecule kinetic analysis of actin filament capping. Polyphosphoinositides do not dissociate capping proteins. *J. Biol. Chem.* **282**, 28014–28024
- 113 Zimmermann, D., Santos, A., Kovar, D.R. and Rock, R.S. (2015) Actin age orchestrates myosin-5 and myosin-6 run lengths. *Curr. Biol.* **25**, 2057–2062
- 114 Hansen, S.D. and Mullins, R.D. (2010) VASP is a processive actin polymerase that requires monomeric actin for barbed end association. *J. Cell Biol.* **191**, 571–584
- 115 Smith, B.A., Gelles, J. and Goode, B.L. (2014) Single-molecule studies of actin assembly and disassembly factors. *Methods Enzymol.* **540**, 95–117
- 116 Paolo, D., Afanzar, D., Berry, R.M., Di Paolo, D., Afanzar, O. and Armitage, J.P. (2016) Single-molecule imaging of electroporated dye-labelled CheY in live *Escherichia coli*. *Philos. Trans. R. Soc. B. Biol. Sci.* **371**, 20150492

- 117 Fujiwara, T.K., Iwasawa, K., Kalay, Z., Tsunoyama, T.A., Watanabe, Y., Umemura, Y.M. et al. (2016) Confined diffusion of transmembrane proteins and lipids induced by the same actin meshwork lining the plasma membrane. *Mol. Biol. Cell* **27**, 1101–1119
- 118 Umemura, Y.M., Vrljic, M., Nishimura, S.Y., Fujiwara, T.K., Suzuki, K.G.N. and Kusumi, A. (2008) Both MHC class II and its GPI-anchored form undergo hop diffusion as observed by single-molecule tracking. *Biophys. J.* **95**, 435–450
- 119 Anderluh, A., Klotzsch, E., Ries, J., Reismann, A.W.A.F., Weber, S., Fölser, M. et al. (2014) Tracking single serotonin transporter molecules at the endoplasmic reticulum and plasma membrane. *Biophys. J.* **106**, L33–L35
- 120 Anderluh, A., Hofmaier, T., Klotzsch, E., Kudlacek, O., Stockner, T., Sitte, H.H. et al. (2017) Direct PIP2 binding mediates stable oligomer formation of the serotonin transporter. *Nat. Commun.* **8**, 14089
- 121 Hirokawa, N., Noda, Y., Tanaka, Y. and Niwa, S. (2009) Kinesin superfamily motor proteins and intracellular transport. *Nat. Rev. Mol. Cell Biol.* **10**, 682–696
- 122 Gramlich, M.W., Conway, L., Liang, W.H., Labastide, J.A., King, S.J., Xu, J. et al. (2017) Single molecule investigation of kinesin-1 motility using engineered microtubule defects. *Sci. Rep.* **7**, 44290
- 123 Von Forster, T.H. (1946) Energiewanderung und Fluoreszenz. *Naturwissenschaften* **33**, 166–175
- 124 Hussain, S.A. (2012) An introduction to fluorescence resonance energy transfer (FRET). *Sci. J. Phys.* **2012**, 4
- 125 König, I., Zarrine-Afsar, A., Aznauryan, M., Soranno, A., Wunderlich, B., Dingfelder, F. et al. (2015) Single-molecule spectroscopy of protein conformational dynamics in live eukaryotic cells. *Nat. Methods* **12**, 773–779
- 126 Dyla, M., Andersen, J.L., Kjaergaard, M., Birkedal, V., Terry, D.S., Altman, R.B. et al. (2016) Engineering a prototypic P-type ATPase *Listeria monocytogenes* Ca²⁺-ATPase 1 for single-molecule FRET studies. *Bioconjug. Chem.* **27**, 2176–2187
- 127 Ticaú, S., Friedman, L.J., Champasa, K., Corrêa, Jr, I.R., Gelles, J. and Bell, S.P. (2017) Mechanism and timing of Mcm2-7 ring closure during DNA replication origin licensing. *Nat. Struct. Mol. Biol.* **24**, 309–315
- 128 Wu, W.-Q., Hou, X.-M., Zhang, B., Fossé, P., René, B., Mauffret, O. et al. (2017) Single-molecule studies reveal reciprocating of WRN helicase core along ssDNA during DNA unwinding. *Sci. Rep.* **7**, 43954
- 129 Birkedal, V., Dong, M., Golas, M.M., Sander, B., Andersen, E.S., Gothelf, K.V. et al. (2011) Single molecule microscopy methods for the study of DNA origami structures. *Microsc. Res. Tech.* **74**, 688–698
- 130 Stein, I.H., Steinhauer, C. and Tinnefeld, P. (2011) Single-molecule four-color FRET visualizes energy-transfer paths on DNA origami. *J. Am. Chem. Soc.* **133**, 4193–4195
- 131 Boersma, A.J., Zuhorn, I.S. and Poolman, B. (2015) A sensor for quantification of macromolecular crowding in living cells. *Nat. Methods* **12**, 227–229
- 132 Freikamp, A., Mehlich, A., Klingner, C. and Grashoff, C. (2017) Investigating piconewton forces in cells by FRET-based molecular force microscopy. *J. Struct. Biol.* **197**, 37–42
- 133 Fijen, C., Montón Silva, A., Hochkoepler, A. and Hohlbein, J. (2017) A single-molecule FRET sensor for monitoring DNA synthesis in real time. *Phys. Chem. Chem. Phys.* **19**, 4222–4230
- 134 Castello, F., Paredes, J.M., Ruedas-Rama, M.J., Martin, M., Roldan, M., Casares, S. et al. (2017) Two-step amyloid aggregation: sequential lag phase intermediates. *Sci. Rep.* **7**, 40065
- 135 Axelrod, D., Koppel, D.E., Schlessinger, J., Elson, E. and Webb, W.W. (1976) Mobility measurement by analysis of fluorescence photobleaching recovery kinetics. *Biophys. J.* **16**, 1055–1069
- 136 Mudumbi, K.C., Schirmer, E.C., Yang, W., Flyvbjerg, H. and Cherry, R.J. (2016) Single-point single-molecule FRAP distinguishes inner and outer nuclear membrane protein distribution. *Nat. Commun.* **7**, 12562
- 137 Wu, M.M., Covington, E.D. and Lewis, R.S. (2014) Single-molecule analysis of diffusion and trapping of STIM1 and Orai1 at endoplasmic reticulum-plasma membrane junctions. *Mol. Biol. Cell* **25**, 3672–3685
- 138 Groeneweg, F.L., van Royen, M.E., Fenz, S., Keizer, V.I.P., Geverts, B., Prins, J. et al. (2014) Quantitation of glucocorticoid receptor DNA-binding dynamics by single-molecule microscopy and FRAP. *PLoS ONE* **9**, e90532
- 139 Arimoto, K., Löchte, S., Stoner, S.A., Burkart, C., Zhang, Y., Miyauchi, S. et al. (2017) STAT2 is an essential adaptor in USP18-mediated suppression of type I interferon signaling. *Nat. Struct. Mol. Biol.* **24**, 279–289
- 140 Tran-Ba, K.-H., Higgins, D.A. and Ito, T. (2015) Fluorescence recovery after photobleaching and single-molecule tracking measurements of anisotropic diffusion within identical regions of a cylinder-forming diblock copolymer film. *Anal. Chem.* **87**, 5802–5809
- 141 Rust, M.J., Bates, M. and Zhuang, X. (2006) Sub-diffraction-limit imaging by stochastic optical reconstruction microscopy (STORM). *Nat. Methods* **3**, 793–796
- 142 Hess, S.T., Girirajan, T.P.K. and Mason, M.D. (2006) Ultra-high resolution imaging by fluorescence photoactivation localization microscopy. *Biophys. J.* **91**, 4258–4272
- 143 Betzig, E., Patterson, G.H., Sougrat, R., Lindwasser, O.W., Olenych, S., Bonifacino, J.S. et al. (2005) Excitation strategies for optical lattice microscopy. *Opt. Express* **13**, 3021–3036
- 144 Chen, C., Zong, S., Wang, Z., Lu, J., Zhu, D., Zhang, Y. et al. (2016) Imaging and intracellular tracking of cancer-derived exosomes using single-molecule localization-based super-resolution microscope. *ACS Appl. Mater. Interfaces* **8**, 25825–25833
- 145 Jiang, H., English, B.P., Hazan, R.B., Wu, P. and Ovryn, B. (2015) Tracking surface glycans on live cancer cells with single molecule sensitivity. *Ang. Chem. Int. Ed. Engl.* **54**, 1765–1769
- 146 Tobin, S.J., Cacao, E.E., Hong, D.W.W., Terenius, L., Vukojevic, V. and Jovanovic-Taliman, T. (2014) Nanoscale effects of ethanol and naltrexone on protein organization in the plasma membrane studied by photoactivated localization microscopy (PALM). *PLoS ONE* **9**, e87225
- 147 Nan, X., Collisson, E.A., Lewis, S., Huang, J., Tamgüney, T.M., Liphardt, J.T. et al. (2013) Single-molecule superresolution imaging allows quantitative analysis of RAF multimer formation and signaling. *Proc. Natl. Acad. Sci. U.S.A.* **110**, 18519–18524

- 148 Jonas, K.C., Fanelli, F., Huhtaniemi, I.T. and Hanyaloglu, A.C. (2015) Single molecule analysis of functionally asymmetric G protein-coupled receptor (GPCR) oligomers reveals diverse spatial and structural assemblies. *J. Biol. Chem.* **290**, 3875–3892
- 149 Belyy, V., Shih, S.-M., Bandaria, J., Huang, Y., Lawrence, R.E., Zoncu, R. et al. (2017) PhotoGate microscopy to track single molecules in crowded environments. *Nat. Commun.* **8**, 13978
- 150 Hu, C.-D., Chinenov, Y. and Kerppola, T.K. (2002) Visualization of Interactions among bZIP and Rel Family Proteins in Living Cells Using Bimolecular Fluorescence Complementation. *Mol. Cell* **9**, 789–798
- 151 Nickerson, A., Huang, T., Lin, L.-J. and Nan, X. (2014) Photoactivated localization microscopy with bimolecular fluorescence complementation (BiFC-PALM) for nanoscale imaging of protein-protein interactions in cells. *PLoS ONE* **9**, e100589
- 152 Nan, X., Tamgüney, T.M., Collisson, E.A., Lin, L.-J., Pitt, C., Galeas, J. et al. (2015) Ras-GTP dimers activate the Mitogen-Activated Protein Kinase (MAPK) pathway. *Proc. Natl. Acad. Sci. U.S.A.* **112**, 7996–8001
- 153 Gröger, P., Poulsen, N., Klemm, J., Kröger, N. and Schlierf, M. (2016) Establishing super-resolution imaging for proteins in diatom biosilica. *Sci. Rep.* **6**, 36824
- 154 Shtengel, G., Galbraith, J.A., Galbraith, C.G., Lippincott-Schwartz, J., Gillette, J.M., Manley, S. et al. (2009) Interferometric fluorescent super-resolution microscopy resolves 3D cellular ultrastructure. *Proc. Natl. Acad. Sci. U.S.A.* **106**, 3125–3130
- 155 Dani, A., Huang, B., Bergan, J., Dulac, C. and Zhuang, X. (2010) Superresolution imaging of chemical synapses in the brain. *Neuron* **68**, 843–856
- 156 Holden, S.J., Pengo, T., Meibom, K.L., Fernandez Fernandez, C., Collier, J. and Manley, S. (2014) High throughput 3D super-resolution microscopy reveals Caulobacter crescentus in vivo Z-ring organization. *Proc. Natl. Acad. Sci. U.S.A.* **111**, 4566–4571
- 157 Chen, Y., Gu, M., Gunning, P.W. and Russell, S.M. (2016) Dense small molecule labeling enables activator-dependent STORM by proximity mapping. *Histochem. Cell Biol.* **146**, 255–266
- 158 Récamier, V., Izeddin, I., Bosanac, L., Dahan, M., Proux, F. and Darzacq, X. (2014) Single cell correlation fractal dimension of chromatin: a framework to interpret 3D single molecule super-resolution. *Nucleus* **5**, 75–84
- 159 Wisniewski, J., Hajj, B., Chen, J., Mizuguchi, G., Xiao, H., Wei, D. et al. (2014) Imaging the fate of histone Cse4 reveals *de novo* replacement in S phase and subsequent stable residence at centromeres. *Elife* **3**, e02203
- 160 Schermelleh, L., Heintzmann, R. and Leonhardt, H. (2010) A guide to super-resolution fluorescence microscopy. *J. Cell Biol.* **190**, 165
- 161 Maldonado, H., Calderon, C., Burgos-Bravo, F., Kobler, O., Zuschratter, W., Ramirez, O. et al. (2017) Astrocyte-to-neuron communication through integrin-engaged Thy-1/CBP/Csk/Src complex triggers neurite retraction via the RhoA/ROCK pathway. *Biochim. Biophys. Acta* **1864**, 243–254
- 162 Abadía-Molina, F., Morón-Calvente, V., Baird, S.D., Shamim, F., Martín, F. and MacKenzie, A. (2017) Neuronal apoptosis inhibitory protein (NAIP) localizes to the cytokinetic machinery during cell division. *Sci. Rep.* **7**, 39981
- 163 Mitchell-Jordan, S., Chen, H., Franklin, S., Stefani, E., Bentolila, L.A. and Vondriska, T.M. (2012) Features of endogenous cardiomyocyte chromatin revealed by super-resolution STED microscopy. *J. Mol. Cell Cardiol.* **53**, 552–558
- 164 Reindl, J., Girst, S., Walsh, D.W.M., Greubel, C., Schwarz, B., Siebenwirth, C. et al. (2017) Chromatin organization revealed by nanostructure of irradiation induced γ H2AX, 53BP1 and Rad51 foci. *Sci. Rep.* **7**, 40616
- 165 Cseresnyes, Z., Schwarz, U. and Green, C.M. (2009) Analysis of replication factories in human cells by super-resolution light microscopy. *BMC Cell Biol.* **10**, 88
- 166 Kinoshita, Y., Kalir, T., Dottino, P., Kohtz, D.S. and Tachibana, T. (2012) Nuclear distributions of NUP62 and NUP214 suggest architectural diversity and spatial patterning among nuclear pore complexes. *PLoS ONE* **7**, e36137
- 167 Schwentker, M.A., Bock, H., Hofmann, M., Jakobs, S., Bewersdorf, J., Eggeling, C. et al. (2007) Wide-field subdiffraction RESOLFT microscopy using fluorescent protein photoswitching. *Microsc. Res. Tech.* **70**, 269–280
- 168 Testa, I., Urban, N.T., Jakobs, S., Eggeling, C., Willig, K.I. and Hell, S.W. (2012) Nanoscopy of living brain slices with low light levels. *Neuron* **75**, 992–1000
- 169 Grotjohann, T., Testa, I., Reuss, M., Brakemann, T., Eggeling, C., Hell, S.W. et al. (2012) rsEGFP2 enables fast RESOLFT nanoscopy of living cells. *Elife* **1**, e00248
- 170 Hoyer, P., de Medeiros, G., Balázs, B., Norlin, N., Besir, C., Hanne, J. et al. (2016) Breaking the diffraction limit of light-sheet fluorescence microscopy by RESOLFT. *Proc. Natl. Acad. Sci. U.S.A.* **113**, 3442–3446
- 171 Balzarotti, F., Eilers, Y., Gwosch, K.C., Gynnå, A.H., Westphal, V., Stefani, F.D. et al. (2017) Nanometer resolution imaging and tracking of fluorescent molecules with minimal photon fluxes. *Science* **355**, 606–612
- 172 Bailey, B., Farkas, D.L., Taylor, D.L. and Lanni, F. (1993) Enhancement of axial resolution in fluorescence microscopy by standing-wave excitation. *Nature* **366**, 44–48
- 173 Zhang, T., Osborn, S., Brandow, C., Dwyre, D., Green, R., Lane, S. et al. (2013) Structured illumination-based super-resolution optical microscopy for hemato- and cyto-pathology applications. *Anal. Cell Pathol. (Amst.)* **36**, 27–35
- 174 Cogger, V.C., McNerney, G.P., Nyunt, T., DeLeve, L.D., McCourt, P., Smedsrød, B. et al. (2010) Three-dimensional structured illumination microscopy of liver sinusoidal endothelial cell fenestrations. *J. Struct. Biol.* **171**, 382–388
- 175 Komis, G., Mistrik, M., Samajová, O., Doskočilová, A., Ovečka, M., Illés, P. et al. (2014) Dynamics and organization of cortical microtubules as revealed by superresolution structured illumination microscopy. *Plant Physiol.* **165**, 129–148
- 176 Pavani, S.R.P., Thompson, M.A., Biteen, J.S., Lord, S.J., Liu, N., Twieg, R.J. et al. (2009) Three-dimensional, single-molecule fluorescence imaging beyond the diffraction limit by using a double-helix point spread function. *Proc. Natl. Acad. Sci. U.S.A.* **106**, 2995–2999
- 177 Creech, M.K., Wang, J., Nan, X., Gibbs, S.L., Baker, M., Cejas, P. et al. (2017) Super-resolution imaging of clinical formalin fixed paraffin embedded breast cancer with single molecule localization microscopy. *Sci. Rep.* **7**, 40766
- 178 Wang, G., Hauver, J., Thomas, Z., Darst, S.A. and Pertsinidis, A. (2016) Single-molecule real-time 3D imaging of the transcription cycle by modulation interferometry. *Cell* **167**, 1839.e21–1852.e21

- 179 Herrmannsdörfer, F., Flottmann, B., Nanguneri, S., Venkataramani, V., Horstmann, H., Kuner, T. et al. (2017) 3D d STORM imaging of fixed brain tissue. *Synapse Development*, pp. 169–184, Springer, New York
- 180 Weisenburger, S., Boening, D., Schomburg, B., Giller, K., Becker, S., Griesinger, C. et al. (2017) Cryogenic optical localization provides 3D protein structure data with Angstrom resolution. *Nat. Methods* **14**, 141–144
- 181 von Diezmann, A., Shechtman, Y. and Moerner, W.E. (2017) Three-dimensional localization of single molecules for super-resolution imaging and single-particle tracking. *Chem. Rev.* **117**, 7244–7275
- 182 Chen, B.-C., Legant, W.R., Wang, K., Shao, L., Milkie, D.E., Davidson, M.W. et al. (2014) Lattice light-sheet microscopy: imaging molecules to embryos at high spatiotemporal resolution. *Science* **346**, 1257998
- 183 Legant, W.R., Shao, L., Grimm, J.B., Brown, T.A., Milkie, D.E., Avants, B.B. et al. (2016) High-density three-dimensional localization microscopy across large volumes. *Nat. Methods* **13**, 359–365
- 184 Sharonov, A. and Hochstrasser, R.M. (2006) Wide-field subdiffraction imaging by accumulated binding of diffusing probes. *Proc. Natl. Acad. Sci. U.S.A.* **103**, 18911–18916
- 185 Jungmann, R., Steinhauer, C., Scheible, M., Kuzyk, A., Tinnefeld, P. and Simmel, F.C. (2010) Single-molecule kinetics and super-resolution microscopy by fluorescence imaging of transient binding on DNA origami. *Nano Lett.* **10**, 4756–4761
- 186 Jungmann, R., Avendaño, M.S., Woehrstein, J.B., Dai, M., Shih, W.M. and Yin, P. (2014) Multiplexed 3D cellular super-resolution imaging with DNA-PAINT and Exchange-PAINT. *Nat. Methods* **11**, 313–318
- 187 Paturzo, M., Merola, F., Grilli, S., De Nicola, S., Finizio, A. and Ferraro, P. (2008) Super-resolution in digital holography by a two-dimensional dynamic phase grating. *Opt. Express* **16**, 17107
- 188 Liu, C., Liu, Z., Bo, F., Wang, Y. and Zhu, J. (2002) Super-resolution digital holographic imaging method. *Appl. Phys. Lett.* **81**, 3143–3145
- 189 Wilson, L.G., Carter, L.M. and Reece, S.E. (2013) High-speed holographic microscopy of malaria parasites reveals ambidextrous flagellar waveforms. *Proc. Natl. Acad. Sci. U.S.A.* **110**, 18769–18774
- 190 Ortega-Arroyo, J. and Kukura, P. (2012) Interferometric scattering microscopy (iSCAT): new frontiers in ultrafast and ultrasensitive optical microscopy. *Phys. Chem. Chem. Phys.* **14**, 15625
- 191 Arroyo, J.O., Andrecka, J., Spillane, K.M., Billington, N., Takagi, Y., Sellers, J.R. et al. (2014) Label-free, all-optical detection, imaging, and tracking of a single protein. *Nano Lett.* **14**, 2065–2070
- 192 Andrecka, J., Takagi, Y., Mickolajczyk, K.J., Lippert, L.G., Sellers, J.R., Hancock, W.O. et al. (2016) Interferometric scattering microscopy for the study of molecular motors. *Methods Enzymol.* **581**, 517–539
- 193 Andrecka, J., Ortega Arroyo, J., Lewis, K., Cross, R.A. and Kukura, P. (2016) Label-free imaging of microtubules with sub-nm precision using interferometric scattering microscopy. *Biophys. J.* **110**, 214–217
- 194 Andrecka, J., Ortega Arroyo, J., Takagi, Y., de Wit, G., Fineberg, A., MacKinnon, L. et al. (2015) Structural dynamics of myosin 5 during processive motion revealed by interferometric scattering microscopy. *Elife* **4**, e05413
- 195 Mickolajczyk, K.J., Deffenbaugh, N.C., Arroyo, J.O., Andrecka, J., Kukura, P. and Hancock, W.O. (2015) Kinetics of nucleotide-dependent structural transitions in the kinesin-1 hydrolysis cycle. *Proc. Natl. Acad. Sci. U.S.A.* **112**, E7186–E7193
- 196 Sarkar, A., Robertson, R.B. and Fernandez, J.M. (2004) Simultaneous atomic force microscope and fluorescence measurements of protein unfolding using a calibrated evanescent wave. *Proc. Natl. Acad. Sci. U.S.A.* **101**, 12882–12886
- 197 He, Y., Lu, M., Cao, J. and Lu, H.P. (2012) Manipulating protein conformations by single-molecule AFM-FRET nanoscopy. *ACS Nano* **6**, 1221–1229
- 198 Bharadwaj, M., Strohmeyer, N., Colo, G.P., Helenius, J., Beerwinkel, N., Schiller, H.B. et al. (2017) αV -class integrins exert dual roles on $\alpha 5\beta 1$ integrins to strengthen adhesion to fibronectin. *Nat. Commun.* **8**, 14348